Final Report

Review of MgO-Related Uncertainties in the Waste Isolation Pilot Plant

Contract Number EP-D-05-002
Work Assignment No. 4-02, TD No. 2008-3
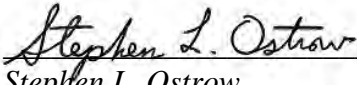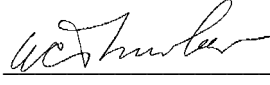

Prepared for:

U.S. Environmental Protection Agency
Office of Radiation and Indoor Air
1310 L Street N.W.
Washington, DC 20005

Charles O. Byrum
Work Assignment Manager

Prepared by:

S. Cohen & Associates
1608 Spring Hill Road
Suite 400
Vienna, Virginia 22182

January 24, 2008

S. Cohen & Associates:	Document No.
	WA 4-02, TD2008-3
Regulatory, Analytical, and Evaluation Support Services *for Radiation Protection Programs*	Effective Date:
	January 24, 2008
Work Assignment 4-02: Technical Support for *Continuing Compliance of the WIPP*	
Review of MgO-Related Uncertainties in the **Waste Isolation Pilot Plant**	Supersedes:
	N/A

Work Assignment Project Manager:

_____   Date   January 24, 2008
Abe Zeitoun

Work Assignment QA Manager:

_____   Date   January 24, 2008
Stephen L. Ostrow

Work Assignment Task Manager:

_____   Date   January 24, 2008
William Thurber

Technical Specialist:

_____   Date   January 24, 2008
Janet Schramke

Revision Log

Revision No.	Date	Description	Affected Sections

TABLE OF CONTENTS

LIST OF TABLES

ABBREVIATION/ACRONYM LIST

AMWTP	Advanced Mixed Waste Treatment Project
CCA	Compliance Certification Application
CCDF	Complementary cumulative distribution function
CDF	Cumulative distribution function
CFR	*Code of Federal Regulations*
CO_2	Carbon dioxide
CPR	Cellulosics, plastics and rubber
CRA	Compliance Recertification Application
DOE	U.S. Department of Energy
DRZ	Disturbed Rock Zone
EDTA	Ethylenediaminetetraacetic acid
EEF	Effective Excess Factor
EF	Excess Factor (equivalent to Safety Factor)
EPA	U.S. Environmental Protection Agency
ERDA-6	Energy Research and Development Administration, simulated Castile brine formulation
FMT	Fracture-Matrix Transport
g	Moles of CO_2 produced per mole of consumed organic carbon
GWB	Generic Weep Brine, simulated Salado brine formulation
LOI	Loss on ignition
m	Fraction of MgO available for CO_2 consumption
M_c	Moles of organic carbon in the CPR emplaced in the repository reported by DOE
$\hat{M}_C$	Moles of organic carbon in the CPR emplaced in the repository
M_{CO2}	Maximum moles of CO_2 that could be generated by microbial consumption of all CPR carbon
MgO	Magnesium oxide
M_{MgO}	Total moles of MgO emplaced in the repository
μ_{CPR}	Average proportion of CPR mass in inventory to amount tracked by DOE
μ_{CPR-C}	Average proportion of moles of CPR carbon in inventory to moles calculated using chemical composition assumptions of Wang and Brush (1996)
μ_{L2B}	Average fraction of MgO lost to brine that flows out of the repository
μ_{RC}	Average concentration of reactive constituents in WTS-60 MgO

μ_{ss}	Average mass of MgO in a disposal room relative to the reported value
PA	Performance assessment
PABC	Performance Assessment Baseline Calculation
PAVT	Performance Assessment Verification Test
PDF	Probability density function
pmH	$-\log_{10}$ of the hydrogen ion molality
PVC	Polyvinylchloride
r	Moles of CO_2 consumed per mole of emplaced MgO
RTR	Real-time radiography
σ_{CPR}	Uncertainty in proportion of CPR mass in inventory to amount tracked by DOE
σ_{CPR-C}	Uncertainty in proportion of moles of CPR carbon in inventory to moles calculated using chemical composition assumptions of Wang and Brush (1996)
σ_{EEF}	Uncertainty in the calculated Effective Excess Factor
σ_{L2B}	Uncertainty in fraction of MgO lost to brine that flows out of the repository
σ_{RC}	Uncertainty in fraction of reactive constituents in WTS-60 MgO
σ_{ss}	Uncertainty in mass of MgO in a disposal room relative to the reported value
σ_{yield}	Uncertainty in moles of CO_2 produced per mole of consumed CPR carbon
TRU	Transuranic
VE	Visual examination
WIPP	Waste Isolation Pilot Plant
y_{CPR}	Parameter representing the ratio of the CPR mass in inventory to amount tracked by DOE
y_{CPR-C}	Parameter representing the ratio of the moles of CPR in inventory to moles calculated using chemical composition assumptions of Wang and Brush (1996)
y_{L2B}	Uncertain parameter representing the fraction of MgO lost to brine
y_{RC}	Uncertain parameter representing the reactive fraction of MgO
y_{SS}	Relative uncertainty in the amount of MgO in a disposal room
y_{yield}	Uncertain parameter representing the moles of CO_2 produced per mole of consumed carbon in the repository; includes effects of precipitated carbonate phases other than magnesite or hydromagnesite

EXECUTIVE SUMMARY

The Waste Isolation Pilot Plant (WIPP) is an underground transuranic (TRU) waste disposal facility operated by the U.S. Department of Energy (DOE) under the oversight of the U.S. Environmental Protection Agency (EPA). Cellulosic, plastic, and rubber (CPR) materials are part of the WIPP waste inventory and are used as waste packaging materials and for waste emplacement. These CPR materials could be microbially degraded during the 10,000-year WIPP regulatory period, producing carbon dioxide (CO_2) and other gases. Elevated CO_2 concentrations in the repository could increase actinide solubilities by reducing brine pH and by forming aqueous actinide carbonate complexes. Excess CO_2 generation could also increase gas pressures in the post-closure repository. Anhydrous, granular, bulk magnesium oxide (MgO) has been included as an engineered barrier in WIPP to mitigate these possible effects. The MgO backfill fulfills the repository design requirement for an engineered barrier "to prevent or substantially delay the movement of water or radionuclides toward the accessible environment" [40 CFR 194.44(a)]. The MgO backfill is expected to react with CO_2, reducing gas pressures, as well as buffering pH and decreasing CO_2 concentrations so actinide solubilities are constrained.

EPA originally calculated the Safety Factor (also referred to by DOE as the Excess Factor or EF) for the MgO backfill as the moles of MgO in the backfill divided by the moles of CPR carbon in the repository. This Excess Factor was equal to 1.95 (EPA 1997). The EF decreased to 1.67 when the MgO minisacks were no longer placed with the waste (EPA 2001). DOE submitted a Planned Change Request in April 2006 to reduce the MgO EF from its current value of 1.67 to 1.20 (Moody 2006). In response, EPA requested additional information about the uncertainties related to the effectiveness of the MgO engineered barrier, the size of these uncertainties, and their potential impacts on WIPP's long-term performance.

DOE responded with an analysis of the uncertainties associated with the effectiveness of MgO, and provided an assessment of the effects of these uncertainties on the calculation of the required quantities of MgO (Vugrin et al. 2006). Vugrin et al. (2006) divided these uncertainties into four categories:

- Uncertainties in the quantity of CPR that will be consumed

- Uncertainties associated with the quantities of CO_2 produced by microbial degradation of CPR

- Uncertainties related to the amount of MgO available to react with CO_2

- Uncertainties in the moles of CO_2 consumed per mole of available MgO, and in the moles of CO_2 that could be consumed by reaction with other materials

To incorporate uncertainties associated with the performance of the MgO backfill, Vugrin et al. (2006) used the Effective Excess Factor (EEF), defined as follows:

$$EEF = \frac{(m \times M_{MgO})}{(g \times M_c)} \times r$$

where:

    g = fraction of CO_2 produced per mole of consumed organic carbon
    m = fraction of MgO available for CO_2 consumption
    M_c = total moles of organic carbon in the emplaced CPR reported by DOE
    M_{MgO} = total moles of MgO emplaced in the repository
    r = moles of CO_2 consumed per mole of emplaced MgO

Vugrin et al. (2006) provided a summary of the uncertainties associated with calculating the excess amounts of MgO relative to the amount required to react with CO_2 and control chemical conditions in the WIPP repository. This summary and the characterization of the uncertainties and their effects on the excess MgO calculations provided a reasonable approach for addressing the uncertainties. The mean value of the EEF calculated by Vugrin was 1.60, indicating that on average, 60% more MgO would be available to consume CO_2 than the amount required.

A review of Vugrin et al. (2006) and supporting information indicated the need for additional data and further analysis of some issues. In response, Vugrin et al. (2007) provided a revised evaluation of the EEF. Because of uncertainty regarding the long-term degradation of CPR, Vugrin et al. (2006, 2007) made the bounding assumption that all CPR could degrade during the 10,000-year WIPP regulatory period. Uncertainty in the CPR inventory masses was accounted for using the results of an evaluation by Kirchner and Vugrin (2006). The results of this study indicated that the mean CPR quantity in a disposal room is expected to equal the sum of the CPR quantities reported by DOE for the individual containers. This study also indicated that the standard deviation would be relatively small because of the random nature of the differences between the reported and actual inventory contents.

The reported masses of CPR in the inventory must be converted to moles of carbon to determine the amount of CO_2 that could be produced by CPR degradation. These calculations require assumptions regarding the chemical composition of the CPR. Assumptions summarized by Wang and Brush (1996) have been used in the past to perform these calculations. Vugrin et al. (2006, 2007) did not consider the possible effects of these assumptions on the EEF. Reasonable estimates of the compositions of the CPR were used by the author of this report to develop reasonable upper-range and lower-range estimates of the moles of carbon in the CPR inventory. Using these estimates, it was determined that the estimated moles of CPR carbon in the inventory ranged from 0.97 to 1.09 times the value calculated using the Wang and Brush (1996) assumptions. This range should be included in the EEF calculations as an uncertain parameter with a uniform distribution.

Vugrin et al. (2006, 2007) assumed that sufficient sulfate was present in the waste, brines, and Salado minerals for complete degradation of all CPR carbon in the repository through sulfate reduction and denitrification. Because of the lower CO_2 yield from the methanogenic CPR degradation reactions, this assumption conservatively bounds the uncertainties related to the microbial reactions that may degrade CPR in the repository.

The WTS-60 MgO that is currently being used as backfill has been reasonably well characterized. Preliminary hydration data provided by Wall (2005) indicates the WTS-60 MgO will likely hydrate and carbonate more rapidly than MgO from previous suppliers. DOE has

proposed hydration and carbonation experiments that would be expected to provide additional information regarding the reactivity of this material; in particular, by providing carbonation data for the WTS-60 MgO. The current specifications (WTS 2005) are unlikely to identify MgO shipments with reactive fractions less than the fraction (96 ± 2 mole %) used in the EEF evaluation. Information regarding the production process and feedstock materials for the WTS-60 MgO has indicated that the variability of different shipments should be relatively low. Because of the high chemical purity of the WTS-60 MgO, it is likely that the WTS-60 MgO will consistently have the reactivity specified in the EEF calculation.

There is no evidence that significant physical segregation of MgO by room roof collapse will occur. Similarly, the MgO supersacks appear very likely to rupture and expose MgO to any brine that enters the repository. The analysis presented by Clayton and Nemer (2006) of loss of MgO with brine from the repository is consistent with previous evaluations of the effects of drilling events on repository performance, and the effects of MgO loss to brine are likely to be relatively small. A very small fraction of the MgO appears likely to carbonate before emplacement, and was accounted for in the EEF calculation. Only a small amount of MgO dissolved in Salado brine is likely to enter the repository and react with CO_2, reducing the required amount of MgO; this effect was conservatively omitted from the calculations. Formation of impermeable rims of reaction products on individual periclase [MgO(s)] grains and impermeable reaction rinds on the masses of MgO in the repository would have the potential to limit the availability of MgO for complete reaction. The possible formation of such reaction rims on individual periclase grains or impermeable rinds on masses of MgO was previously considered by the Conceptual Models Peer Review Panel (Wilson et al. 1996a, 1996b, 1997a, 1997b). The Panel concluded that formation of magnesium-carbonate reaction products would not inhibit the access of brine to the surfaces of the MgO and would not render any of the MgO unavailable for reaction with brine and CO_2. No new data have been developed since the time of this review to contradict this assumption; consequently, it is reasonable to continue to assume that essentially all MgO in the backfill will be available for reaction with brine and CO_2. Kanney and Vugrin (2006) evaluated aqueous diffusion of CO_2 in the repository; their results indicate that the repository will be sufficiently well mixed to permit contact and reaction of the MgO with brine and CO_2.

Upon reaction with brine, periclase in the backfill is expected to hydrate to brucite [$Mg(OH)_2(s)$]. In the presence of CO_2, brucite can react to form magnesite [$MgCO_3(s)$], the most stable magnesium-carbonate phase, or a metastable magnesium-carbonate phase, such as hydromagnesite [$Mg_5(CO_3)_4(OH)_2 \cdot 4H_2O(s)$]. The formation of brucite and a magnesium-carbonate phase in the repository is expected to control both pH and CO_2 fugacities within ranges consistent with relatively low and predictable actinide solubilities in repository brines. Under WIPP repository conditions, hydromagnesite is expected to form first, with eventual reaction to form the more stable magnesite phase. The rate at which hydromagnesite will convert to magnesite is important, because it affects the moles of CO_2 consumed per mole of MgO reacted, which in turn affects the EEF calculation. Examination of experimental and natural analogue data indicated that the hydromagnesite to magnesite reaction rate could be relatively slow, so this reaction may not be complete during the WIPP repository regulatory period. Consequently, Vugrin et al. (2007) used an uncertain variable with a uniform

distribution to represent the moles of CO_2 consumed per mole of reacted MgO. This variable ranged from 0.8 (hydromagnesite only) to 1.0 (magnesite only).

Significant amounts of CPR degradation by sulfate reduction would require dissolution of sulfate minerals in the Salado Formation, including anhydrite $[CaSO_4(s)]$, gypsum $[CaSO_4 \bullet 2H_2O(s)]$, and polyhalite $[K_2MgCa_2(SO_4)_4 \bullet 2H_2O]$. Dissolution of these solid phases would release relatively large quantities of calcium ion into the brine. Elevated calcium concentrations would, in turn, be expected to cause calcium-carbonate precipitation and increased consumption of CO_2 per mole of MgO in the backfill. DOE carried out EQ3/6 geochemical calculations to estimate the proportions of CO_2 that would be consumed by magnesite or hydromagnesite and calcium carbonate precipitation; however, limitations in the EQ3/6 thermodynamic database resulted in modeling calculations that inadequately represented repository conditions. Because of the difficulties associated with quantifying the amount of calcium-carbonate solids that would precipitate, the limiting assumption was made for the EEF calculation that no calcium carbonate precipitation would occur. This is undoubtedly a conservative, bounding assumption, and will lead to an underestimation of the EEF.

Vugrin et al. (2007) calculated a mean EEF of 1.03, with a standard deviation of 0.0719. Incorporating the effects of uncertainty associated with the chemical composition of the CPR would reduce the EEF to 1.00, with a standard deviation of 0.078. This EEF would seem to indicate that if the EF is reduced to 1.20, the average amount of MgO in a disposal room would equal the quantity required to react with CO_2. The EEF calculation, however, includes a number of conservative assumptions, including the assumptions that all CPR will degrade, all carbon in the CPR will react to form CO_2, and carbonate minerals other than hydromagnesite or magnesite will not precipitate, including calcite, iron carbonates, or lead carbonates. Given these conservative, bounding assumptions, it is likely that if the EF is changed to 1.20, the EEF in the disposal rooms will be greater than the average bounding value of 1.00. Consequently, reduction of the EF to 1.20 is likely to have no significant effects on repository chemistry.

Changes to the conceptual models that relate to repository chemistry from the time of the Compliance Certification Application Performance Assessment Verification Test to the present have been relatively minor. These conceptual models have evolved since the time of the original certification decision because of the availability of additional information about processes such as microbial degradation and complexation of actinides by organic ligands. At this time, the available data related to repository performance are consistent with the current chemistry-related conceptual models, and the conceptual models appear to adequately represent expected conditions in the repository.

Langmuir (2007) performed an independent technical review of a draft version of the present report. The comments provided by Langmuir (2007) were considered and additional information was incorporated in the final version of the present report to address the issues raised in the review. Detailed information supporting the responses to the review comments provided by Langmuir (2007) is provided in SCA (2008).

1.0   INTRODUCTION

The Waste Isolation Pilot Plant (WIPP) is an underground transuranic (TRU) waste disposal facility located in southeastern New Mexico. The WIPP facility is operated by the U.S. Department of Energy (DOE) under the oversight of the U.S. Environmental Protection Agency (EPA). In 1998, DOE received certification for operation of WIPP from EPA, based on a review of the Compliance Certification Application (CCA) and supporting information, including the Performance Assessment Verification Test (PAVT) (EPA 1998a). After receiving this certification, DOE began accepting TRU waste for disposal in March 1999. EPA recertified WIPP operations in March 2006, based on EPA's review of the 2004 Compliance Recertification Application (CRA-2004) and supporting information, including the Performance Assessment Baseline Calculation (PABC) (EPA 2006a).

Cellulosic, plastic, and rubber (CPR) are part of the WIPP waste inventory; cellulosic and plastic materials are also used for waste packaging and for waste emplacement. Microbial degradation of CPR during the 10,000-year WIPP regulatory period could affect repository performance by producing carbon dioxide (CO_2) and other gases. Elevated CO_2 concentrations in the repository could increase actinide solubilities in repository brines by reducing brine pH and by forming aqueous actinide carbonate complexes. To limit the potential effects of CO_2 generation, anhydrous, granular, bulk magnesium oxide (MgO) has been included as the only engineered barrier in WIPP. The MgO backfill fulfills the repository design requirement for an engineered barrier "to prevent or substantially delay the movement of water or radionuclides toward the accessible environment" [40 CFR 194.44(a)]. The MgO backfill is expected to react with CO_2, buffering pH and decreasing CO_2 concentrations so that actinide solubilities are constrained. The MgO backfill is also expected to reduce gas pressures in the post-closure repository by reacting with gaseous CO_2. Gas pressures in the repository are expected to affect predicted radionuclide releases; for example, lower gas pressures should result in lower spallings releases.

DOE originally proposed placing the MgO backfill in the repository as 4,000-lb "supersacks" positioned on top of each waste stack, with 25-lb "minisacks" placed around the waste containers. At the time of the CCA, EPA calculated the Safety Factor for the MgO backfill in the entire repository as the moles of MgO in the backfill divided by the moles of CPR carbon. This Safety Factor was equal to 1.95 (EPA 1997). EPA (2001) later approved DOE's proposal to discontinue use of the MgO minisacks to improve worker safety. When the MgO minisacks were no longer placed with the waste, the calculated Safety Factor decreased to 1.67 (EPA 2001). DOE currently uses MgO supersacks weighing 4,200 lbs in the repository (WTS 2005).

DOE requested approval from EPA to place compressed waste from the Advanced Waste Treatment Project (AMWTP) in the WIPP repository (Triay 2002). A concern associated with compressed AMWTP waste was that relatively high CPR densities in this waste could decrease the Safety Factor. The request to emplace the compressed waste was approved by EPA, with the requirement that DOE ensure that the Safety Factor equaled or exceeded the approved value of 1.67 (Marcinowski 2004). To comply with this requirement, DOE began calculating the Safety Factor for each room in the repository as it was filled, adding additional MgO to each room, if necessary, to ensure that the Safety Factor was 1.67 or higher (Detwiler 2004).

DOE and EPA documents prepared for the CCA and CRA-2004 used the term "Safety Factor" for the ratio of the moles of MgO to the moles of CPR carbon in the repository. Recent DOE documents (e.g., Vugrin et al. 2006, 2007), however, have referred to this ratio as the Excess Factor (EF), defined as follows:

$$EF = \frac{M_{MgO}}{M_{CO2}} \times 1 \text{ mole of } CO_2 \text{ consumed/1 mole of MgO} \qquad (1)$$

where:

M_{MgO} = total moles of emplaced MgO

M_{CO2} = the maximum possible number of moles of CO_2 that could be generated by microbial consumption of all carbon in the CPR

Vugrin et al. (2006, 2007) stated that the EF is equivalent to the Safety Factor. To be consistent with DOE's current nomenclature, EF is used in the remainder of this report.

DOE submitted a Planned Change Request to EPA to reduce the MgO EF from the approved value of 1.67 to 1.20 (Moody 2006). In response to this request, EPA noted the importance of the MgO backfill as WIPP's only engineered barrier (Gitlin 2006). EPA observed that during the original certification decision, it was assumed that excess MgO would compensate for potential uncertainties related to chemical reactions in the repository. Because DOE was proposing a lower EF, EPA requested additional information about the uncertainties related to MgO effectiveness, the size of these uncertainties, and their potential impacts on WIPP's long-term performance.

DOE responded to this request with an analysis of the uncertainties associated with the effectiveness of MgO, and provided an assessment of the effects of these uncertainties on the calculation of required MgO quantities (Vugrin et al. 2006). Vugrin et al. (2006) divided these uncertainties into four categories:

- Uncertainties in the quantity of CPR that will be consumed

- Uncertainties associated with the quantities of CO_2 produced by microbial degradation of CPR

- Uncertainties related to the amount of MgO available to react with CO_2

- Uncertainties in the moles of CO_2 consumed per mole of available MgO, and in the moles of CO_2 that could be consumed by reaction with other materials

To evaluate the uncertainties associated with the performance of the MgO backfill, Vugrin et al. (2006) defined the Effective Excess Factor (EEF) as follows:

$$EEF = \frac{\left(m \times M_{MgO}\right)}{\left(g \times M_c\right)} \times r \qquad (2)$$

where:

g = uncertainty in the moles of CO_2 produced per mole of consumed organic carbon

m = uncertainty in the moles of MgO available for CO_2 consumption

M_c = total moles of organic carbon in the emplaced CPR reported by DOE

r = uncertainty in the moles of CO_2 consumed per mole of emplaced MgO

Vugrin et al. (2006) addressed the uncertainties associated with the parameters in Equation (2). The Vugrin et al. (2006) report and supporting documentation were reviewed to determine whether DOE had adequately accounted for uncertainties associated with the performance of the MgO engineered barrier. During this review, EPA requested additional information related to the proposed change in the MgO EF. DOE presented this additional information to EPA during technical exchange meetings in September 2006, January 2007, and May 2007. DOE then provided a revised report describing the uncertainties associated with the MgO EF in the repository (Vugrin et al. 2007).

The revised information provided by Vugrin et al. (2007) has been reviewed. In Section 2.0 of this report, the uncertainties associated with CO_2 production are evaluated. Section 3.0 addresses the uncertainties associated with the availability of MgO in the repository, and Section 4.0 addresses uncertainties related to the consumption of CO_2. The EEF calculations are reviewed and modified in Section 5.0. The chemistry-related conceptual models for WIPP are reviewed in Section 6.0 to determine whether these models continue to adequately represent expected repository conditions. The conclusions of this review are provided in Section 7.0. The results of this review indicate that reducing the EF from 1.67 to 1.20 is unlikely to significantly affect WIPP repository chemistry, based on the available information.

Langmuir (2007) performed an independent technical review of a draft version of the present report. The comments provided by Langmuir (2007) were considered and additional information was incorporated in the final version of the present report to address the issues raised in the review. More detailed information supporting the responses to comments provided by Langmuir (2007) is provided in SCA (2008).

2.0   CARBON DIOXIDE PRODUCTION

Production of CO_2 in the repository will depend on the CPR inventory, the amounts of CPR materials that degrade, and the reactions by which the materials degrade. Vugrin et al. (2006, 2007) represented CO_2 production in the repository using the following equation:

$$\text{moles of } CO_2 = y_{yield} \times y_{CPR} \times M_c \tag{3}$$

In this equation, y_{yield} is an uncertain parameter related to the moles of CO_2 produced per mole of consumed carbon in the repository; this term also includes the effects of CO_2 consumption by phases other than magnesite $[MgCO_3(s)]$[1] or hydromagnesite $[Mg_5(CO_3)_4(OH)_2 \bullet 4H_2O(s)]$. The parameter y_{CPR} represents uncertainty associated with the moles of CPR carbon emplaced in the repository. The parameters y_{yield} and y_{CPR} were used to represent the parameter g in Equation (2). The sources of uncertainties related to CO_2 production are discussed below.

2.1   CELLULOSIC, PLASTIC, AND RUBBER INVENTORY

Vugrin et al. (2007) related the reported amount of CPR in WIPP waste (M_c) to the amount actually present in the repository ($\hat{M}_c$):

$$\hat{M}_c = y_{CPR} \times M_c \tag{4}$$

The total inventory of CPR in the repository includes materials in the waste; packaging materials, such as drum liners; and emplacement materials, such as polyethylene slip sheets used to support the MgO supersacks. The CPR inventory is calculated using information about wastes that have been emplaced in WIPP, and information about stored and anticipated (projected) wastes (Leigh et al. 2005a). The inventory of CPR waste and emplacement materials is reported in terms of the masses of (1) cellulosic materials, including paper, cloth, and wood; (2) plastic materials, including polyethylene and polyvinylchloride (PVC); and (3) rubber materials, such as neoprene and Hypalon®.

Kirchner and Vugrin (2006) examined the uncertainties associated with the mass of CPR in the inventory. In this analysis, they compared CPR estimates obtained using real-time radiography (RTR) for 200 drums to CPR estimates for the same drums based on visual examination (VE). The results showed no significant bias. Although relatively large differences between the VE and RTR measurements were observed for some individual drums, these errors did not significantly affect the total CPR inventory in a room, because of the random nature of the differences between the two sets of measurements. Kirchner and Vugrin (2006) found that the uncertainty associated with the mass of CPR in a disposal room would be no more than 0.3%. SCA (2006b) performed a technical review of the information presented by Kirchner and Vugrin (2006). SCA (2006b) determined that there was a relatively small bias in the RTR versus VE measurements, with RTR slightly underestimating the VE values. However, this bias was found to have negligible effects on the calculated uncertainty of approximately 0.2% for CPR in a room (SCA 2006b).

---

[1] As part of a chemical formula, (s) indicates a solid phase.

Vugrin et al. (2006) set the mean value of y_{CPR} equal to 1, consistent with the conclusion that the mean CPR quantity in a room will equal the sum of the CPR quantities in the individual containers reported by DOE. The standard deviation, σ_{CPR}, was set equal to 0.003, the upper bound on the relative uncertainty associated with the amount of CPR in a single room (Vugrin et al. 2006). This formulation of the y_{CPR} parameter and relative uncertainty is consistent with the available data.

The reported mass of CPR in the inventory must be converted to moles of carbon for the calculation of the amount of CO_2 that could be produced by CPR degradation. This calculation was carried out for the CCA and CRA-2004 using assumptions about the nature of the materials that make up the CPR. The assumptions about the chemical composition of the CPR were described by Wang and Brush (1996):

(1) The chemical composition of all cellulosics could be approximated by cellulose monomer ($C_6H_{10}O_5$)

(2) Plastics in the inventory were 80% polyethylene and 20% PVC

(3) Rubber in the waste was 50% neoprene and 50% Hypalon®

Using these assumptions, Vugrin et al. (2006) calculated that the total reported WIPP CPR carbon inventory (M_c) was 1.1×10^9 moles; however, this value did not include the moles of carbon from emplacement cellulosics and plastics. The correct total CPR carbon inventory in the repository based on PABC information and the assumptions of Wang and Brush (1996) is 1.21×10^9 moles (Leigh et al. 2005b), an increase of about 10% over the values used by Vugrin et al. (2006).

Vugrin et al. (2006, 2007) did not consider the possible effects of the CPR chemical composition assumptions on the EEF calculations. Wang and Brush (1996) assumed that the cellulosic materials present in the repository could be approximated by the chemical formula for cellulose monomer ($C_6H_{10}O_5$). Using this formula, approximately 44% of cellulosic materials are carbon by weight (Table 1). Using the chemical composition of cellulose is reasonable for materials such as cotton cloth, because it is nearly 100% cellulose (Lynd et al. 2002). However, wood is composed of cellulose, hemicellulose, and lignin, with an overall elemental composition of about 50% carbon, 6% hydrogen, 44% oxygen, and trace amounts of several metal ions (Pettersen 1984). Using this elemental composition, wood contains 41.6 moles of carbon/kg, whereas cellulose contains 37.0 moles carbon/kg. As a consequence, use of the cellulose monomer formula for all cellulosic materials could lead to a slight underestimation of the amount of carbon in the cellulosic material inventory.

Wang and Brush (1996) assumed that plastic materials in the WIPP waste and emplacement materials were 80% polyethylene and 20% PVC. Other plastics reported in the repository waste and emplacement materials include polypropylene from the MgO supersacks, polystyrene (Styrofoam^{TM}), plexiglass (Lucite®) and Teflon® (DOE 2004, Appendix DATA). Polyethylene has a relatively high carbon concentration (Table 1), so assuming that polyethylene comprises the majority of the plastics would tend to maximize the estimated carbon content of the plastics inventory.

Wang and Brush (1996) assumed that rubber in the WIPP waste is composed of 50% Hypalon® and 50% neoprene. In addition to these materials, the presence of latex gloves is commonly noted in the inventory descriptions (DOE 2004, Appendix DATA). If the composition of the latex gloves is approximately equal to that of isoprene, the presence of latex could slightly increase the carbon content of the rubber in the inventory over the estimated value (Table 1).

Table 1.   Compositions of Cellulosic, Plastic, and Rubber Materials

Material	Monomer formula	Moles carbon per kilogram
Cellulose	$C_6H_{10}O_5$	37.0
Wood	not available	41.6
Polyethylene	C_2H_4	71.3
Polyvinylchloride	C_2H_3Cl	32.0
Polypropylene	C_3H_6	71.3
Polystyrene	C_8H_8	76.8
Plexiglass	$C_5O_2H_8$	49.9
Teflon®	C_2F_4	20.0
Hypalon®	$(C_7H_{13}Cl)_{12}\text{-}(CHSO_2Cl)_{17}$	28.8
Neoprene	C_4H_5Cl	45.2
Latex (isoprene)	C_5H_8	73.4

The relative amounts of CPR carbon in the WIPP inventory were calculated using the assumptions outlined by Wang and Brush (1996), and inventory and waste emplacement materials information reported for the PABC (SCA 2006a). Results of these calculations indicated that the majority of the CPR carbon would be present as plastics (61%) and cellulosics (32%), with only a minor amount (7%) present in the form of rubber materials. As a result, the chemical compositions of the materials in the plastics and cellulosics will be the most likely to affect the amount of CPR carbon in the repository that could degrade and form CO_2.

Because of the nature of WIPP waste, the exact proportions of materials in the CPR inventory cannot be quantified. Limiting assumptions could be used to calculate the maximum and minimum amount of CPR carbon in the inventory. For example, to calculate the maximum amount of carbon that could be present, it could be assumed that all cellulosics are wood; all plastics, besides the polyethylene and polypropylene packaging and emplacement materials, are polystyrene; and all rubber is isoprene. However, such a calculation would be inconsistent with what is known about the WIPP inventory. For example, although it is known that polyethylene and polypropylene are present in large quantities in the inventory, packaging, and emplacement materials, other plastics such as PVC, Teflon® and plexiglass are present in the waste, and these materials have lower carbon concentrations by weight.

To determine the possible effects of different CPR compositions on predicted total CPR carbon in the repository, the following assumptions were made to produce a reasonable upper-range estimate:

(1) Cellulosic wastes are composed of 50% cellulose and 50% wood. This proportion accounts for the presence of wood and the composition of paper, which is likely to be intermediate between that of wood and pure cellulose.

(2) Plastic wastes are 90% polyethylene and polypropylene, and the remainder is composed of equal percentages (2.5%) of PVC, polystyrene, plexiglass, and Teflon®.

(3) Rubber wastes consist of equal proportions (33.3%) of Hypalon®, neoprene, and isoprene.

Using these assumptions and the compositions listed in Table 1, a reasonable upper-range estimate for the total moles of CPR carbon in the inventory is 1.32×10^9 moles. This value represents an increase of approximately 9% over the CPR carbon inventory calculated using the Wang and Brush (1996) assumptions.

To provide a reasonable lower estimate for the total moles of CPR carbon in the repository, the following assumptions were made:

(1) Cellulosic wastes are composed of 75% cellulose and 25% wood.

(2) Because of the polyethylene and polypropylene used for waste packaging and emplacement, the minimum percentage of these materials in the plastics inventory will be 37.4%, based on the PABC inventory. Therefore, plastics are assumed to be 60% polyethylene and polypropylene, 20% PVC, and the remainder made up of equal percentages (6.7%) of polystyrene, plexiglass and Teflon®.

(3) Rubber wastes consist of 45% each of Hypalon® and neoprene, and 10% isoprene.

These assumptions and the compositions listed in Table 1 yielded a lower-range estimate of 1.18×10^9 moles of CPR carbon in the inventory. This value is about 3% lower than the CPR carbon value calculated using the Wang and Brush (1996) assumptions.

Thus, if M_c is the moles of carbon reported to be in the CPR inventory, calculated using the assumptions of Wang and Brush (1996), the uncertainty in $\hat{M}_C$ can be represented by the following:

$$\hat{M}_C = y_{CPR} \times y_{CPR-C} \times M_c \tag{5}$$

In this equation, y_{CPR-C} is a parameter representing the ratio of the moles of CPR carbon in the waste to the moles calculated using the assumptions of Wang and Brush (1996). The CPR carbon inventories calculated using the different assumptions about the chemical composition of the wastes fall within a range of 0.97 to 1.09 times the moles of CPR carbon calculated using the assumptions of Wang and Brush (1996), and provide a reasonable range for the value of y_{CPR-C}. The mean value of y_{CPR-C} is 1.03, and because there is little information about the precise chemical composition of the CPR, the uncertainty of y_{CPR-C} should be represented by a uniform distribution.

2.2 CELLULOSIC, PLASTIC, AND RUBBER DEGRADATION PROBABILITY

The probability of CPR degradation in the WIPP repository was qualitatively addressed by Vugrin (2006, 2007). The information considered by Vugrin et al. (2006, 2007) was previously presented by Brush (1995, 2004) and evaluated by EPA (2006b) during the CRA-2004 evaluation. The conclusion of EPA's previous evaluation was that at least some microbial degradation of CPR is likely to occur.

The potential CPR degradation reactions that could occur within the WIPP repository and the possible extent of these reactions during the 10,000-year regulatory period were examined in SCA 2006a. It was concluded that cellulosic materials were relatively likely to be microbially degraded in the repository environment if sufficient brine is available. However, plastics and rubber materials are likely to degrade relatively slowly, and might not degrade completely during the repository regulatory period. Uncertainties associated with the degradation rates of plastics and rubber in the repository include the potential effects of long-term radiolysis on the extent of biodegradation of these materials, and whether short-term aerobic radiolysis and biodegradation reactions could affect long-term degradability of plastic and rubber in the repository.

Because of the uncertainties associated with the likely extent of CPR degradation in the repository environment, Vugrin et al. (2006, 2007) assumed for the EEF calculations that all CPR would be microbially degraded. This assumption is bounding, in that it provides a maximum estimate of the amount of CO_2 that could be generated by microbial degradation of CPR.

2.3 CARBON DIOXIDE YIELD

Vugrin et al. (2006) included both CO_2 production by CPR degradation and CO_2 consumption by precipitation of carbonate phases other than magnesite and hydromagnesite in the calculation of the term y_{yield}. The value of y_{yield} depends on the microbial degradation and carbonate precipitation reactions in the repository, and the upper limit on y_{yield} is 1. If a fraction of the CPR carbon is degraded to form compounds other than CO_2, or if carbonate phases other than magnesite or hydromagnesite precipitate, then the CO_2 yield would be less than 1. The potential precipitation of calcite [$CaCO_3(s)$] and its inclusion in y_{yield} is discussed in Section 4.0, along with other reactions that may remove CO_2 from repository brines.

In the Gas Generation conceptual model developed for the CCA that was also used for the CRA, it was assumed that the major pathways for microbial degradation of CPR are the following reactions:

$$C_6H_{10}O_5 + 4.8\ H^+ + 4.8\ NO_3^- \rightarrow 7.4\ H_2O + 6\ CO_2 + 2.4\ N_2 \tag{6}$$
$$C_6H_{10}O_5 + 6\ H^+ + 3\ SO_4^{2-} \rightarrow 5\ H_2O + 6\ CO_2 + 3\ H_2S \tag{7}$$
$$C_6H_{10}O_5 + H_2O \rightarrow 3\ CH_4 + 3\ CO_2 \tag{8}$$
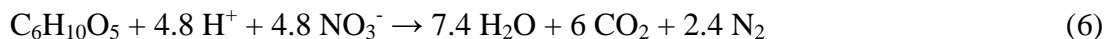
In these reactions, $C_6H_{10}O_5$ is the assumed chemical formula for cellulose. In (6) and (7), referred to respectively as the denitrification and sulfate reduction reactions, one mole of CO_2 is produced for each mole of organic carbon consumed. Therefore, if all CPR degradation occurs

through these reactions, the CO_2 produced per mole of CPR carbon will equal 1. On the other hand, the methanogenesis reaction (8) produces only 0.5 moles of CO_2 per mole of CPR carbon consumed. Significant amounts of CPR degradation via reaction (8) would result in a CO_2 yield between 0.5 and 1. Another methanogenesis reaction occurs in the natural environment in addition to reaction (8); this methanogenesis reaction is as follows:

$$4 H_2 + CO_2 \rightarrow CH_4 + 2 H_2O \tag{9}$$

This is commonly referred to as the CO_2 reduction pathway (Chapelle 1993). Reaction (9) consumes CO_2 and could significantly reduce y_{yield} if it occurred in the WIPP repository. It is uncertain whether methanogenesis would be more likely to occur by reactions (8) or (9).

Methanogenic microbes that could degrade CPR via reactions (8) and (9) typically predominate in subsurface environments where other electron acceptors, such as nitrate (NO_3^-) and sulfate (SO_4^{2-}), are absent and reactions (6) and (7) cannot occur (Chapelle 1993). Relatively limited amounts of nitrate and sulfate are present in the WIPP waste inventory, which would be expected to result in methanogenesis if the waste was the only possible source of electron acceptors for the CPR degradation reactions. However, sulfate is present in the Salado and Castile brines, as well as in minerals present in the Salado Formation surrounding the repository, including anhydrite ($CaSO_4$), gypsum [$CaSO_4 \bullet 2H_2O$] and polyhalite [$K_2MgCa_2(SO_4)_4 \bullet 2H_2O$]. Vugrin et al. (2006, 2007) assumed that sufficient sulfate was present in the waste, brines, and Salado minerals for complete degradation of all CPR carbon in the repository through sulfate reduction. This assumption is consistent with the Chemical Conditions conceptual model, which includes the assumption that brines remain in equilibrium with anhydrite. Because of the lower CO_2 yield from the methanogenesis reactions (8) and (9), this assumption conservatively bounds the uncertainties related to the microbial reactions that may degrade CPR in the repository.

3.0 MAGNESIUM OXIDE AVAILABILITY IN THE REPOSITORY

The performance of MgO as an engineered barrier will depend on the physical and chemical characteristics of the MgO, and whether it is available to react with brine and CO_2. DOE provided additional information regarding these issues to support its Planned Change Request to reduce the MgO EF to 1.20.

3.1 CHARACTERIZATION OF MAGNESIUM OXIDE

Three different sources of MgO have been used since WIPP waste emplacement began in March 1999 (Brush and Roselle 2006). Magnesium oxide was provided by National Magnesia Chemicals from March 1999 to mid-April 2000, and by Premier Chemicals from mid-April 2000 to December 2004 or January 2005. Since that time, MgO has been provided by Martin Marietta Magnesia Specialties LLC (Martin Marietta). Only the characteristics of MgO being supplied by Martin Marietta now and in future shipments are directly relevant to the requested change in the MgO EF. However, some of the available data on MgO chemical reactivity were obtained using MgO from other sources, and these data were considered where appropriate.

The MgO currently being emplaced in the WIPP repository is referred to by the supplier as MagChem® 10 WTS-60 MgO.[2] The typical chemical composition of this material and the material specifications reported by the supplier are summarized in Table 2; more detailed chemical data are provided in Appendix A. Analysis of a shipment of WTS-60 MgO indicated that 100% passed through a 9.5 mm (3/8th inch) sieve (Martin Marietta 2006), which meets the specification that 99.5% should pass through this sieve size (WTS 2005). WTS-60 MgO was initially characterized by Wall (2005), with additional, more detailed characterization data reported by Deng et al. (2006a).

Table 2.   Reported Chemical Composition of Martin Marietta WTS-60 Magnesium Oxide[3]

Constituent	Typical WTS-60 Composition (Martin Marietta) wt %	Specifications wt %	Average Chemical Analysis (Martin Marietta) wt %		Chemical Analysis (Deng et al. 2006a) wt %
			12/1/2004 to 12/1/2005	6/1/2006 to 5/31/2007	
MgO	98.2	97.0 minimum	98.5 ± 0.166	98.5 ± 0.169	98.5 ± 2.5
CaO	0.9	1.0 maximum	0.904 ± 0.112	0.904 ± 0.107	0.874 ± 0.025
SiO_2	0.4	0.5 maximum	0.349 ± 0.075	0.348 ± 0.088	0.311 ± 0.008
Fe_2O_3	0.2	0.3 maximum	0.162 ± 0.022	0.154 ± 0.029	0.115 ± 0.009
Al_2O_3	0.1	0.2 maximum	0.125 ± 0.024	0.134 ± 0.014	0.130 ± 0.018
Total	99.8	--	100.0	100.0	99.9

---

[2] MagChem®10 is the Martin Marietta designation for hard-burned, high-purity, technical grades of MgO processed from magnesium-rich brines. WTS-60 is a grade specially formulated to meet DOE specifications.
[3] Stated uncertainties are $\pm 1\sigma$.

The WTS-60 MgO characterized by Wall (2005) had a bulk density of 87 lb/ft^3, equal to the specified minimum of 87 ± 5 lb/ft^3 (WTS 2005). Wall (2005) performed hydration tests at 90ºC to determine the rate of brucite [Mg(OH)$_2$(s)] formation from WTS-60 MgO and other MgO samples. These samples may also have formed small quantities of portlandite [Ca(OH)$_2$(s)] from lime [CaO] present as an impurity in the MgO. The amount of brucite plus portlandite formed during the hydration tests was determined through loss on ignition (LOI) of the reacted samples at 500ºC and 750ºC. Based on the LOI tests at 500ºC, Wall (2005) found that the WTS-60 MgO contained 90 ± 3 mole % reactive periclase [MgO(s)]. Loss on ignition tests could not be performed successfully at 750ºC with the WTS-60 MgO, because of sample decrepitation at this temperature. However, comparison of LOI results at 500ºC and 750ºC using hydrated samples of Premier MgO or another Martin Marietta MgO sample (WTS-30) indicated that the 500ºC LOI results underestimated the amount of brucite plus portlandite by approximately 4 to 9 mole %.

Deng et al. (2006a) reported a chemical analysis of WTS-60 MgO performed at Sandia National Laboratories (Table 2); Martin Marietta reported analyses of samples performed for two different time periods (Table 2 and Appendix A). The MgO and CaO reported in the chemical analyses represent all magnesium and calcium present in the material, including magnesium and calcium incorporated into relatively unreactive phases, such as silicates. To determine the amounts of reactive periclase and lime in the WTS-60 MgO, Deng et al. (2006a) performed LOI and thermogravimetric tests on WTS-60 samples that had been hydrated at 90ºC for at least 3 days. Deng et al. (2006a) used the chemical analysis results, the LOI, and thermogravimetric results that indicated the weights of water in the hydrated WTS-60 MgO, and reasonable assumptions regarding the nonreactive phases in the MgO to calculate the amounts of reactive periclase and lime. The results indicated that the WTS-60 MgO contained 96 ± 2 (1σ) mole % reactive periclase plus lime, with periclase making up 95 mole % and lime making up 1 mole % of the WTS-60 MgO. Vugrin et al. (2006) used the random variable y_{RC} to represent the reactive fraction of the MgO placed in the repository, with a mean of 0.96 and a standard deviation (σ_{RC}) of 0.02, based on the Deng et al. (2006a) results.

Carbonation rate data are not available for the WTS-60 MgO. DOE has proposed to carry out experimental studies of the hydration and carbonation of WTS-60 MgO (Deng et al. 2006b). The results of these investigations are not yet available. However, results of hydration experiments reported by Wall (2005) indicate that WTS-60 MgO hydrates more rapidly than Premier MgO, and the chemical analysis results of Deng et al. (2006a) indicate that WTS-60 MgO contains a higher percentage of reactive periclase plus lime than Premier MgO. Pending the results of the proposed experiments, it is reasonable to assume that WTS-60 MgO will be as effective for controlling CO$_2$ fugacities and pH in repository brines as Premier MgO, and may be more effective.

The WTS-60 MgO sample tested by Deng et al. (2006a) was found to contain 96 ± 2 mole % reactive periclase plus lime. This mean and uncertainty were based on LOI and thermogravimetric analysis of eight samples from a single shipment; Deng et al. (2006a) did not provide information regarding the possible variability between different shipments of this material. The feedstock characteristics and manufacturing process for the WTS-60 MgO may provide some indication of its potential physical and chemical variability. Brush and Roselle

(2006) described the process used to manufacture the WTS-60 MgO from brine and dolomitic limestone. The materials used to manufacture the MgO are calcium-magnesium-chloride brine and dolomitic limestone. Martin Marietta calcines the dolomitic limestone to produce a CaO-MgO solid called dolime. The dolime is mixed with the brine and water to obtain a slurry of brucite plus a calcium-chloride solution. The brucite solid is separated from the solution and washed to remove the calcium chloride and other brine solution components. The brucite is then calcined at 1,000ºC to 1,500ºC (hard-burned) to produce MgO.

Patterson (2007) provided additional information regarding the brine, dolime, and production process for the MagChem® 10 WTS-60 material. The brine is obtained from the Filer Sandstone in Michigan. The brine reservoir extends over 300 square miles and the Martin Marietta wells span 40 square miles of this area. The cations in this chloride brine primarily consist of calcium and magnesium, with minor concentrations of sodium, potassium, and strontium. The $MgCl_2$ concentration in the brine is approximately 10% on a mass basis. The production wells have different concentrations of the various constituents, so Martin Marietta mixes water from the wells to maintain a constant brine composition in their feedstock. The brine reservoir in Martin Marietta's operating area is relatively large, and only about 25% of the brine has been depleted during more than 50 years of operation. Consequently, a stable brine source is anticipated for the foreseeable future. Martin Marietta provided brine feedstock chemistry data from 2004 to mid-2007, which roughly corresponds to the period that WTS-60 has been used as WIPP backfill (Appendix A). The chemistry of the brine has been relatively stable, with average annual $MgCl_2$ concentrations ranging from 107 to 110 g/liter, with annual standard deviations of 3 to 5 g/liter.

Martin Marietta also provided a summary of the calcined dolomitic limestone (dolime) feedstock chemistry from 2004 to mid-2007 (Appendix A). The concentrations of MgO and CaO in this material remained constant at average values of 40.4 ± 0.214 (1σ) wt % and 58.2 ± 0.335 (1σ) wt %, respectively. Martin Marietta has ample reserves of the dolomitic limestone feedstock, and expects these reserves will last in excess of 45 years. Chemical analysis of 146 samples of the WTS-60 MgO over one year (mid-2006 to mid-2007) yielded an average MgO of 98.5 ± 0.085 (1σ) wt %, with CaO as the largest impurity at less than 1 wt % (Table 2).

The information about the chemical processes and feedstock for the production of the WTS-60 MgO indicates that the composition of the feedstock materials has been and is likely to remain relatively constant. The available chemical data for the WTS-60 MgO used for the WIPP backfill indicates that the total chemical composition, on a wt % basis, has also remained stable.

DOE has established specifications for the MgO backfill (WTS 2005). The specifications related to the chemical composition of the material are as follows:

> *The sum of magnesium oxide (MgO) plus calcium oxide (CaO) shall be a minimum of 95%, with MgO being no less than 90%. The remainder of the material shall not contain any items considered hazardous to people or the environment.*

This specification applies only to the total chemical analysis on a wt % basis and does not directly apply to the reactive portion of the materials, which is expressed in the EEF calculation

on a mole % basis. The reactivity test included in the MgO specifications (WTS 2005, Attachment B) was based on information provided by Krumhansl et al. (1997). It appears unlikely that this specification is sufficient to ensure adequate reactivity of the materials in each MgO shipment. For example, the Premier MgO previously used as backfill passed the reactivity test, but Premier MgO contained only 85 wt % reactive periclase (Snider 2003). However, the high chemical purity and consistency of the feedstock materials and production process for WTS-60 MgO indicates that the chemical reactivity is likely to remain relatively constant over time. Consequently, the Martin Marietta WTS-60 MgO appears likely to meet the performance specification of 96 ± 2 (1σ) mole % reactive MgO and CaO in the EEF calculation, based on the available information.

3.2   MAGNESIUM OXIDE SEGREGATION

If a significant portion of the MgO backfill became segregated from brine and CO_2, MgO hydration and carbonation reactions could be limited and the MgO engineered barrier might not function as designed. Reaction of the MgO backfill with CO_2 is important to WIPP performance assessment under both humid and inundated conditions. Under humid conditions, the amount of brine present in the repository is insufficient for direct brine release. Consequently, the important function of the MgO backfill under humid conditions is to control gas pressures by reaction with most of the CO_2. The Conceptual Models Peer Review Panel concluded that DOE had resolved the issue of MgO reactivity for the purposes of the Gas Generation conceptual model by demonstrating that sufficient access of brine and CO_2 to the MgO would occur to substantially remove CO_2 as a pressure source (Wilson et al. 1996b, Section 3.21.3.3). Consequently, the potential segregation of MgO backfill under humid conditions is of limited concern in this analysis.

The effectiveness of the MgO barrier to control chemical conditions and actinide solubilities is important under inundated conditions, when sufficient brine is available for direct brine release. Under inundated conditions, the MgO must react to control pH and CO_2 partial pressures to limit actinide solubilities. Three possible processes have been identified that could result in the segregation of the reactive periclase in MgO from brine and CO_2: physical segregation by roof collapse; formation of impermeable reaction rims on individual MgO granules by the precipitation of hydration and carbonation reaction products; and formation of cementitious, impermeable reaction rinds on the surfaces of larger masses of MgO.

Vugrin et al. (2006, 2007) considered the potential for physical segregation of MgO from brine by roof collapse. They concluded that segregation of MgO was unlikely because of the following:

- Collapse is most likely to occur by lowering of the roof beam onto the MgO and waste stacks, which would not segregate the MgO

- If collapse of smaller blocks occurs, these blocks would tend to be fractured and permeable to brine

- Small-scale spalling from the roof would be unlikely to segregate MgO

- The current practice of ensuring the EF is maintained in each room minimizes the potential for segregation of MgO from brine

For these reasons, roof collapse is unlikely to cause significant amounts of MgO to be physically segregated from brine and unavailable for reaction with CO_2.

The Conceptual Models Peer Review Panel evaluated the potential formation of impermeable reaction rims on individual MgO granules and the possible effects of such reaction rims on the ability of the MgO backfill to control chemical conditions in the repository (Wilson et al. 1996a, 1996b, 1997a, 1997b). SNL (1997) demonstrated that hydromagnesite would nucleate away from the surface of the periclase grains under inundated repository conditions and that isolating reaction rims would not form. The evidence presented by SNL (1997) and reviewed by the Conceptual Models Peer Review Panel included experimental results, optical microscopy, scanning electron microscopy, modeling predictions, analogue comparisons, and phase equilibria information. Based on their review of this information, the Conceptual Models Peer Review Panel agreed that the formation of reaction rims on hydrated MgO granules would not significantly affect the function of the MgO engineered barrier (Wilson et al. 1997b). EPA (1997) considered the experimental evidence and the Conceptual Models Peer Review Panel's conclusions during their evaluation of the effectiveness of the MgO engineered barrier. EPA (1997) concluded that the reactions would occur as predicted to control chemical conditions in the repository, although EPA also cited as additional justification the large excess of MgO to be placed in the repository.

DOE has continued investigating the reaction of MgO backfill materials with brine and CO_2 (Bryan and Snider 2001a; Bryan and Snider 2001b; Snider 2001; Zhang et al. 2001; Snider 2002; Snider and Xiong 2002; Snider 2003; Xiong and Snider 2003). In the hydration and carbonation experiments performed since the Conceptual Models Peer Review, there has been no evidence of reaction rim formation on MgO granules that would hinder complete reaction. Consequently, the conclusions of the Conceptual Models Peer Review Panel (1997b) remain valid, specifically, that formation of impermeable reaction rims on individual periclase granules is unlikely to significantly affect the amount of MgO backfill available for reaction with brine and CO_2.

The reaction of periclase to form brucite and hydromagnesite results in a significant change in mineral volume; in theory, formation of these reaction products on the outside of the masses of emplaced MgO during initial contact with brine and CO_2 could segregate a significant amount of MgO and prevent complete reaction. This process might not occur in small-scale laboratory experiments; however, it would be difficult to design large-scale MgO hydration and carbonation experiments that reproduce expected repository conditions because of the relatively slow reaction rates and long time frame involved. Consequently, the possible formation of impermeable reaction rinds on the outside of the emplaced MgO packages was evaluated by the Conceptual Models Peer Review Panel (Wilson et al. 1996a, 1996b, 1997a, 1997b).

In response to concerns expressed by the Panel regarding the possible formation of impermeable reaction rinds, Bynum et al. (1996) and SNL (1997) presented data from a series of experiments designed to more closely simulate the brine to MgO ratio anticipated in a partially inundated disposal room. In these experiments, MgO was placed in a porous bag that was partially

suspended in brine and CO_2 was bubbled through the brine. After reaction for up to 25 days, the bag of MgO was removed from the brine and placed into a dye solution for three days. The bag and its contents were then dried, impregnated with plastic, and sectioned. Examination of the reacted material showed that dye penetrated below the base of the reaction product surface layer, indicating that the surface reaction products did not prevent contact between the brine and remaining periclase. Because of the relatively high CO_2 partial pressure used in this series of experiments, the magnesium hydroxycarbonate phase formed was nesquehonite. Hydromagnesite formation is anticipated in the repository because of lower CO_2 partial pressures; hydromagnesite has a looser, more platy crystal morphology (SNL 1997). Based on this morphology, SNL (1997) concluded that hydromagnesite was even less likely to inhibit continued reaction between brine and periclase than nesquehonite. The Conceptual Models Peer Review Panel reviewed the information presented by Bynum et al. (1996) and SNL (1997) and concluded that formation of impermeable reaction rinds on the MgO emplaced in the repository would not prevent the MgO barrier from functioning as designed. Although the expected presence of a large excess of MgO in the repository was noted by the Panel, this information was not cited in support of the Panel's judgment that impermeable reaction rinds would not form on the masses of MgO (Wilson et al. 1997b).

During their CCA review of the MgO backfill performance, EPA accepted DOE's assertion that the formation of reaction products on the surfaces of the backfill material would not have a significant, detrimental impact on the ability of the MgO to maintain predicted repository chemical conditions (EPA 1997). EPA (1997) stated that, based on a review of information in Bynum et al. (1996), "formation of reaction products on the surfaces of the backfill material do(es) not have a significant, detrimental impact on the ability of the MgO to maintain the predicted chemical conditions." EPA (1997) also noted DOE's intention to emplace sufficient MgO backfill in the repository to ensure CO_2 consumption would exceed the rate of CO_2 production.

The possible formation of solid masses of MgO reaction products during hydration under inundated conditions was investigated by DOE in a later series of experiments with 5 to 15 mm-thick layers of MgO backfill material (Snider 2002). Although there was significant scatter in the results, there was no evidence that an impermeable mass of hydration products formed. There is no new evidence since the Conceptual Models Peer Review or the CCA review by EPA that impermeable layers of reaction products will form and prevent the reaction of brine and CO_2 with periclase in the interior of the masses of MgO in the repository. In the absence of new information, the conclusion of the Conceptual Models Peer Review Panel and EPA that this issue has been fully addressed remains valid (Wilson et al. 1997b, EPA 1997).

3.3   LOSS OF MAGNESIUM OXIDE TO BRINE OUTFLOW

MgO dissolved in brine that flows out of the repository in the event of an intrusion would affect the amount of MgO available to react with CO_2. Clayton and Nemer (2006) estimated the amount of MgO that could leave a waste panel due to outflowing brine caused by drilling intrusions. The analysis included a Monte Carlo simulation of 1,000 drilling "futures," modeled as a Poisson process with an assumed human-intrusion drilling rate of 5.25×10^{-3} intrusions per km^2 per year. Using the total berm area of the repository, this translated to an expected rate of

33 intrusions in one 10,000-year drilling future, spaced 300 years apart, on average. This rate includes all intrusions that hit the entire repository footprint defined by the berm; only a fraction of these intrusions actually intersects a waste panel.

Each drilling future thus contains a randomly generated number of drilling intrusion events over the 10,000-year analysis period. The probabilities in Table 3 were used to characterize each intrusion. Approximately 20% of the intrusions were assumed to penetrate waste panels, based on the ratio of panel area to the area of the berm (probability of 0.202 in row 1 of Table 3). The intrusions identified as hitting a waste panel were assigned randomly to one of the 10 panels. The intrusions were also randomly identified as either intersecting or not intersecting a Castile brine pocket, and the boreholes were assigned randomly to being plugged with one of the three standard plug types. After the characteristics of each intrusion were assigned, the intrusions that enter a waste panel were classified as either an E1 intrusion (a brine packet is hit with plug type 2), E2 intrusion (no brine pocket is hit, or brine is hit, but plug type is 3), or determined to have no effect on brine flow. This classification was based on the randomly assigned characteristics of the intrusion (Table 4).

Table 3.   Intrusion Characteristics and Probabilities

Characteristic	Probability
Hit Waste Panel	0.202
Hit Brine Pocket	0.01 – 0.60
Hit Panel 1-10	0.10
Plug Type 1	0.015
Plug Type 2	0.696
Plug Type 3	0.289

Table 4.   Intrusion Classification Matrix

Classification	Hit Waste?	Hit Brine Pocket?	Plug Type
No Change	No	Yes or No	1, 2 or 3
	Yes	Yes or No	1
E1	Yes	Yes	2
E2	Yes	Yes	3
	Yes	No	2 or 3

The CRA-2004 PABC included calculations of three replicates of 100 vectors each (300 total vectors). The results of the PABC calculations included the cumulative volumes of brine expected to flow from the intruded waste panel under the repository conditions for each vector. The amount of MgO that would leave the repository due to E1 and E2 intrusions was calculated using these volumes, with the mass of MgO assumed equivalent to the total MgO solubility in Castile brine (157 moles/m^3) or Salado brine (578 moles/m^3), depending on the release scenario. In this analysis, it was conservatively assumed that no MgO reacts with CO_2 before brine

outflow occurs. The amount of MgO leaving the panel was adjusted for the length of time between the drilling future intrusion and the end of the 10,000-year compliance period. This calculation was performed for all 300 PABC vectors for each of the 1,000 drilling futures. The 300,000 calculated MgO values were summarized using a cumulative distribution function (CDF), complementary cumulative distribution function (CCDF), and probability density function (PDF).

The PDF was used to estimate the average fraction of the available MgO predicted to leave the panel. The average percentage of MgO backfill lost to brine flow out of the panel was calculated to be 0.8 ± 1.9 (1σ) % of the available MgO (Clayton and Nemer 2006). This fraction was calculated using the underestimated CPR carbon inventory (Section 2.1) and an assumed EF of 1.20; Nemer (2007) revised this fraction to 0.7 ± 1.7 (1σ) %, using the corrected CPR carbon inventory and the assumed EF of 1.20. Vugrin et al. (2007) used this mean and standard deviation for the parameters μ_{L2B} and σ_{L2B} to represent the mean and standard deviation of the MgO lost to brine.

3.4   MIXING PROCESSES

Mixing processes in the repository brine will occur through advection, dispersion, and molecular diffusion in the aqueous phase. Aqueous diffusion is likely to be the slowest of these processes. An assessment of the length and time scales of diffusion processes in the repository can provide a conservative analysis of mixing that will allow contact and reaction of CO_2 with MgO in the repository. Wang (2000) calculated the time necessary for aqueous CO_2 diffusion to occur over the expected final repository room heights, using information from the CCA; these calculations were reviewed and summarized by Vugrin et al. (2006). The amount of time necessary for diffusion to occur over the final room heights was less than the expected residence time of the brine, indicating that diffusion alone would be adequate for mixing to occur on the length scales present in the repository. Wang (2000) also calculated a range of characteristic diffusion distances that would be consistent with the expected residence time of brine in the repository. This diffusion distance range equaled or exceeded the range of the expected final room height at closure. Consequently, it was determined that mixing would be adequate to allow reaction of CO_2 with MgO backfill, even in the absence of advective or dispersive processes.

The mixing analysis carried out by Wang (2000) was updated using technical baseline data from the PABC for waste panel porosities, brine flows, and pore volumes (Kanney and Vugrin 2006). Kanney and Vugrin (2006) found that the range of diffusion distances bracketed the range of final room heights, and the characteristic diffusion times were less than the hydraulic residence time. These results indicate that molecular diffusion alone should be sufficient to allow contact and reaction of CO_2 with the MgO backfill in the repository. Because of differences in waste characteristics, Kanney and Vugrin (2006) also evaluated the potential effects of AMWTP compressed waste and pipe overpack waste on calculated diffusion lengths and time scales. The calculations were carried out for various loading schemes, which included different mixtures of standard waste, pipe overpack waste, and AMWTP compressed waste. The range of characteristic diffusion lengths was greater than the range of room heights for all non-standard waste loading scenarios. Characteristic diffusion times were shorter than the residence time for

all non-standard waste loading schemes, which also indicates that molecular diffusion alone should be sufficient for complete mixing in the repository.

EPA (1998b) calculated the change in porosity in a waste disposal room caused by the precipitation of hydromagnesite; the results demonstrated that the overall reduction in porosity caused by hydromagnesite precipitation was likely be only 1.4% of the initial porosity. EPA (1998b) related the permeability to the porosity and concluded that the MgO backfill and its reaction products would be unlikely to significantly affect permeability in the waste region of the repository.

These evaluations of mixing processes in the repository are consistent with the Chemical Conditions conceptual model. The Chemical Conditions model includes the assumptions of chemical homogeneity and solubility equilibrium, and that brine and waste are well mixed. As a consequence of these assumptions, chemical microenvironments are not believed to persist in the repository (Wilson et al. 1996a).

3.5   OTHER FACTORS

Other factors that could affect the amounts of MgO available to react with CO_2 in the repository include the possibility that MgO could carbonate before emplacement, the likelihood that a significant number of supersacks will not rupture, or the uncertainties associated with the amount of MgO in the supersacks. In addition, Salado brine has a magnesium ion concentration of 1.0 M, and this magnesium ion could react with CO_2.

For the CCA, DOE evaluated the ability of MgO supersack materials to prevent carbonation of MgO prior to emplacement, and predicted that less than 0.1% of the MgO would be carbonated by CO_2 penetrating the bag materials over 30 years (Vugrin et al. 2006). Vugrin et al. (2006), therefore, used this fraction of MgO that could be lost to carbonation prior to emplacement in their evaluation of the available MgO backfill.

Supersack rupture is likely to occur through lithostatic loading, which will apply stresses that are hundreds of times greater than the maximum loading specifications for supersack rupture (Vugrin et al. 2006). Microbial degradation of the polyethylene supersacks may also contribute to supersack rupture. Accordingly, it is reasonable to assume that the supersacks will rupture and allow the exposure of all MgO backfill materials to brine and CO_2.

The weight of each MgO supersack is specified for procurement as $4,200 \pm 50$ lbs (WTS 2005). Vugrin et al. (2006) calculated the contribution of the uncertainty in the individual supersack weights to the uncertainty in the MgO in an individual room. The random variable y_{ss} was used to represent the uncertainty in the amount of MgO present in the repository relative to the amount tracked; this random variable had a mean value (μ_{ss}) of 1, because there is no expectation of bias in the weights. The standard deviation (σ_{ss}) of the relative amount of MgO in each room was determined to be 0.00037.

The concentration of magnesium ion in unreacted GWB (Salado) brine is 1.0 M; Vugrin et al. (2007) indicated that assuming that magnesium in the brine would not carbonate has a

conservative effect on the calculation of the EEF. Examination of the concentrations of magnesium in GWB brine before and after equilibration with the MgO backfill under WIPP repository conditions (in equilibrium with hydromagnesite) indicates that the concentration declines from 1.0 M to 0.58 M (EPA 2006a). The maximum volume of Salado brine per panel was calculated as 7,763 m^3, which is equivalent to 7.763×10^7 liters in the 10-panel repository. Consequently, the amount of magnesium that would carbonate in this volume of Salado brine would be 3.26×10^7 moles, which would consume 2.61×10^7 moles of CO_2 through hydromagnesite precipitation. This quantity of CO_2 represents approximately 2.2% of the total CPR carbon in the repository, indicating that neglecting the magnesium ion in the Salado brine is likely to have a relatively minor, conservative effect on the EEF calculation.

3.6   INCORPORATION OF MAGNESIUM OXIDE AVAILABILITY IN EFFECTIVE EXCESS FACTOR CALCULATIONS

DOE calculated the fraction of MgO available to react with CO_2 using the following equation:

$$m = y_{SS} \times y_{RC} \times 0.999 - y_{L2B} \tag{10}$$

In this equation, y_{SS} is an uncertain parameter representing the MgO present in a room relative to the amount tracked by DOE (Section 3.5), y_{RC} is an uncertain parameter that represents the reactive fraction of the MgO (Section 3.1), 0.999 represents the MgO fraction that remains uncarbonated after emplacement (Section 3.5), and y_{L2B} is an uncertain parameter representing the amount of MgO lost to brine outflow (Section 3.3). This formulation includes the reasonable assumptions that mixing processes will be sufficient to allow contact of MgO with CO_2 in the repository, and that the MgO supersacks will rupture and allow contact between the MgO and brine, as discussed in Sections 3.4 and 3.5, respectively.

3.7   SUMMARY OF MAGNESIUM OXIDE AVAILABILITY ISSUES

The WTS-60 MgO backfill material has been reasonably well characterized. Preliminary hydration data provided by Wall (2005) indicate that the WTS-60 MgO will likely hydrate and carbonate more rapidly than MgO from previous suppliers. Proposed hydration and carbonation experiments would provide additional information regarding the reactivity of this material; in particular, by providing carbonation data obtained with the WTS-60 MgO. Information regarding the production process and feedstock for the WTS-60 MgO indicates that the variability of different WTS-60 shipments should be relatively low. The current specifications (WTS 2005) may not adequately identify MgO shipments with reactive fractions less than the fraction (96 ± 2 mole %) specified in the EEF evaluation. However, the consistency of the chemical processes and feedstock materials used to produce the WTS-60 MgO and the high chemical purity of this material indicates that WTS-60 MgO is likely to have a chemical reactivity consistent with the fraction specified in the EEF calculation.

There is no evidence that significant physical segregation of MgO by room roof collapse will occur. After a thorough review of the available data, the Conceptual Models Peer Review Panel and EPA concluded that the formation of reaction rims on periclase granules or cementitious outer layers of reaction products on the emplaced MgO would not be expected to limit the availability of periclase in the MgO for reaction (Wilson et al. 1997b, EPA 1997). The MgO

supersacks appear likely to rupture and expose MgO to brine and CO_2. The analysis presented by Clayton and Nemer (2006) of the likely loss of MgO due to outflowing brine is consistent with previous evaluations of the effects of drilling events on repository performance. The effects of MgO loss to brine are likely to be relatively small, based on the Clayton and Nemer (2006) analysis results. A very small fraction of the MgO appears likely to carbonate before emplacement, and only a relatively small amount of magnesium dissolved in Salado brine is likely to enter the repository and react with CO_2. Kanney and Vugrin (2006) evaluated diffusion in the repository; their results indicate that the repository will be sufficiently well mixed to permit contact and reaction of the MgO with brine and CO_2.

4.0   CARBON DIOXIDE CONSUMPTION

According to the Chemical Conditions conceptual model used for the CCA and CRA-2004, the MgO backfill will react with brine to produce brucite [$Mg(OH)_2(s)$]. The following brucite dissolution reaction is expected to control brine pH at values of approximately 8.5 to 9 (DOE 2004, Appendix PA Attachment SOTERM):

$$Mg(OH)_2(s) + 2\,H^+ \rightarrow Mg^{2+} + 2\,H_2O \tag{11}$$

In the presence of brine and CO_2, brucite can react to form magnesite, the most stable magnesium-carbonate phase, or a metastable hydrous magnesium-carbonate phase, such as hydromagnesite. The formation of brucite and a magnesium-carbonate phase in the repository is expected to control both pH and CO_2 fugacities within ranges consistent with relatively low and predictable actinide solubilities in repository brines.

4.1   MAGNESIUM OXIDE CARBONATION

The temperature in the WIPP repository is expected to remain close to the ambient value of 28ºC (DOE 2004, Appendix PA, Attachment SOTERM). The available thermodynamic data indicate that magnesite is the most stable magnesium carbonate phase at this temperature (Lippmann 1973, Königsberger et al. 1999). However, because of slow nucleation and growth rates of magnesite at low temperatures, metastable hydrous magnesium carbonate phases such as hydromagnesite and nesquehonite [$MgCO_3 \bullet 3H_2O(s)$] are the only magnesium carbonate phases that form in low-temperature laboratory experiments. The relatively low rates of conversion of metastable hydrous magnesium carbonate phases to magnesite at low temperatures have been attributed to the strong bonds between the magnesium ion and its associated waters of hydration (Christ and Hostetler 1970).

Experimental investigations of brucite carbonation and MgO hydration and carbonation reactions carried out with WIPP backfill materials and reagent-grade MgO have indicated that hydromagnesite forms readily under the low CO_2 partial pressure conditions expected in the WIPP repository (Bryan and Snider 2001a, Snider and Xiong 2002, Xiong and Snider 2003). In some experiments carried out at higher CO_2 partial pressures, nesquehonite formed initially, but its conversion to hydromagnesite was observed over time (Snider and Xiong 2002).

Hydromagnesite that forms in the WIPP repository should eventually convert to magnesite. However, the reaction rate at the low temperatures expected in the WIPP repository is uncertain. If hydromagnesite persists in the repository for thousands of years, higher CO_2 fugacities and actinide solubilities would be predicted than if magnesite formation occurs. In addition, hydromagnesite formation would result in the consumption of less CO_2 per mole of reacted MgO than the formation of magnesite.

The number of moles of CO_2 consumed per mole of reacted MgO depends on the chemical formula of hydromagnesite. The hydromagnesite chemical formula has been reported in the literature as both $Mg_5(CO_3)_4(OH)_2 \bullet 4H_2O(s)$ and $Mg_4(CO_3)_3(OH)_2 \bullet 3H_2O(s)$. The moles of CO_2 consumed per mole of MgO for the different formulas are 0.8 and 0.75, respectively. The

consensus in the scientific literature is that the two chemical formulas represent the same phase (e.g., Langmuir 1965, Lippmann 1973). Lippmann (1973) attributed the different formulas to the difficulty of analytically determining the precise ratio of CO_2 and water in the mineral structure. The hydromagnesite chemical formula currently accepted by the International Mineralogical Association is $Mg_5(CO_3)_4(OH)_2 \cdot 4H_2O(s)$ (IMA 2007), and this formula was identified by DOE as the composition of the hydromagnesite formed in the MgO carbonation experiments (DOE 2004). This formula, referred to by DOE (2004) as hydromagnesite$_{5424}$, is the composition assumed for hydromagnesite in the remainder of this report.

The rate at which hydromagnesite will transform to magnesite during the 10,000-year regulatory period will affect the EEF calculation. The formation of magnesite consumes one mole of CO_2 for each mole of magnesium:

$$Mg(OH)_2(s) + CO_2 \rightarrow MgCO_3(s) + H_2O \tag{12}$$

On the other hand, only 0.8 moles of CO_2 are consumed for each mole of magnesium during hydromagnesite formation:

$$5\ Mg(OH)_2(s) + 4\ CO_2 \rightarrow Mg_5(CO_3)_4(OH)_2 \cdot 4H_2O(s) \tag{13}$$
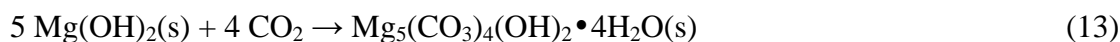
The conversion of hydromagnesite to magnesite presented below consumes additional CO_2, so that the overall ratio of MgO and CO_2 consumed equals one if MgO reacts completely to magnesite:

$$Mg_5(CO_3)_4(OH)_2 \cdot 4H_2O(s) + CO_2 \rightarrow 5\ MgCO_3 + 5\ H_2O \tag{14}$$

Because the rate of conversion of hydromagnesite to magnesite is uncertain, it was assumed that the brucite-hydromagnesite reaction would control CO_2 fugacities for the calculation of actinide solubilities for the CCA PAVT and the CRA PABC (Leigh et al. 2005a).

Brush and Roselle (2006) assumed that the replacement of hydromagnesite by magnesite would occur relatively rapidly, and that magnesite would be the dominant magnesium carbonate phase for most of the 10,000-year WIPP regulatory period. Consequently, Vugrin et al. (2006) assumed that one mole of CO_2 would be consumed per mole of MgO. Brush and Roselle (2006) determined that the conversion of hydromagnesite to magnesite would be relatively rapid under repository conditions, based on the thermodynamic stability of magnesite under WIPP conditions, the presence of magnesite in the Salado Formation, extrapolation of reaction rate data from experiments carried out for WIPP (Zhang et al. 2000), and an evaluation of natural analogue data. The factors considered by Brush and Roselle (2006) are examined below.

4.1.1 Thermodynamic Stability of Magnesite and Its Occurrence in the Salado Formation

As stated at the beginning of Section 4.1, magnesite is expected to be the stable magnesium-carbonate phase under WIPP repository conditions. EPA previously considered the presence of magnesite in the Salado Formation (EPA 1998c). Brush and Roselle (2006) indicated that the presence of magnesite in the Salado is evidence that it will form in the repository as a result of

MgO hydration and carbonation; however, they also stated that there is some ambiguity regarding the origins of this magnesite, and it is uncertain whether the magnesite was formed in situ or was transported as sedimentary material. In addition, the Salado Formation is approximately 200 million years old (Lambert 1992), so the presence of magnesite does not provide insight on the conversion rate of hydromagnesite to magnesite within the 10,000-year WIPP regulatory period. The presence of magnesite in the Salado Formation and the available thermodynamic data indicate that magnesite is likely to remain stable after it forms in the repository, but do not provide information regarding the rate of conversion of hydromagnesite to magnesite.

4.1.2   Experimental Rate Data for the Conversion of Hydromagnesite to Magnesite

Sayles and Fyfe (1973) and Zhang et al. (2000) experimentally investigated the rates at which hydromagnesite converts to magnesite. Because of extremely low reaction rates at low temperatures, reaction-rate experiments were carried out at temperatures of 110ºC to 200 ºC. However, there is evidence that magnesite can form at lower temperatures, because Usdowski (1994) observed magnesite formation in experiments conducted for up to 7 years at temperatures as low as 50 ºC.

Sayles and Fyfe (1973) investigated the conversion of hydromagnesite to magnesite at 126ºC as a function of magnesium ion concentration, CO_2 partial pressure, and ionic strength up to 0.05 M. The results were characterized by an induction period with no detectable crystallization, followed by a period of crystal growth with a fourth-order reaction rate as a function of time. Increased CO_2 partial pressure or an increased hydromagnesite solid-to-solution ratio shortened the induction period, whereas increased $MgCl_2$ concentrations in solution increased the induction period. Increased ionic strength and CO_2 partial pressure increased reaction rates.

Zhang et al. (2000) conducted a series of experiments to determine the conversion rates of reagent-grade hydromagnesite to magnesite plus brucite at 110ºC, 150 ºC, and 200ºC. Experiments were carried out in saturated NaCl and GWB (simulated Salado) brine. In these experiments, the conversion of hydromagnesite to magnesite exhibited an induction period, during which conversion was relatively slow. After approximately 4% to 5% of the hydromagnesite had converted to magnesite plus brucite, more rapid conversion rates were observed. Rates were higher in the NaCl solutions than in GWB brine, and reaction rates increased with temperature. Zhang et al. (2000) determined reaction rate coefficients for the high-growth-rate period by assuming first-order reaction kinetics. An Arrhenius equation was used to extrapolate the rates to 25ºC. Based on the extrapolated data, Zhang et al. (2000) determined half times for the reaction, defined as the time required for half of the hydromagnesite to convert to magnesite plus brucite. These half times were 4.7 years and 73 years in saturated NaCl and GWB, respectively. Zhang et al. (2000) determined conversion rates during the induction periods and used the Arrhenius equation to extrapolate these rates to 25ºC; the resulting 25ºC induction periods were found to be 18 years and 200 years in the NaCl and GWB brines, respectively.

Zhang et al. (2000) performed additional experiments to qualitatively assess the effects of ionic strength, $MgCl_2$ concentrations, and $MgSO_4$ concentrations on the hydromagnesite conversion

rate. These experiments were performed in solutions with various NaCl concentrations, GWB with various $MgCl_2$ concentrations, saturated NaCl solutions with various amounts of $MgCl_2$, and saturated NaCl with various amounts of $MgSO_4$. Increasing ionic strength increased the rate of formation of magnesite in the NaCl solutions, whereas increased magnesium or sulfate concentrations decreased the magnesite formation rate in both the NaCl solution and GWB.

When extrapolated to low temperatures, the results of Zhang et al. (2000) suggest that complete conversion of hydromagnesite to magnesite will occur relatively early during the 10,000-year WIPP regulatory period. However, there are a number of uncertainties associated with this conclusion. For example, the maximum percentage of reaction reported in GWB brine was 77%. Zhang et al. (2000) did not explain why the GWB experiments were not carried out to completion, particularly at 200ºC, where the reaction rate was relatively rapid. Therefore, these data may suggest that complete conversion of hydromagnesite to magnesite may not occur in GWB brine at the rates determined in the experiments. There is also significant uncertainty associated with the extrapolated rates and induction periods. Zhang et al. (2000) pointed out that there were order-of-magnitude uncertainties associated with the induction period calculations because of the small amounts of reaction and uncertainties in the method used to determine reaction extent. In addition, Sayles and Fyfe (1973) observed the following in their discussion of the conversion of hydromagnesite to magnesite:

> *Induction periods are very sensitive to extraneous influences such as impurities and changes in surface area, surface characteristics and solution volume. Where such influences are important, the lengths of observed induction periods are usually not reproducible.*

Because the experiments were not carried out with hydromagnesite created from the hydration and carbonation of MgO backfill materials under WIPP-relevant conditions, it is uncertain whether the induction period measured in the Zhang et al. (2000) experiments would be representative of actual repository conditions. Vugrin et al. (2006) did not incorporate the uncertainties in the induction period in their EEF calculations.

Zhang et al. (2000) demonstrated that assuming a different reaction order, i.e., the fourth-order kinetic equation consistent with the equation used by Sayles and Fyfe (1973), resulted in 25ºC reaction half times of 40,000 years in NaCl and 30,000,000 years in GWB. These results show that the extrapolated rates at 25ºC are sensitive to the assumed form of the rate equation. These uncertainties were not considered in the analysis of Vugrin et al. (2006). The low reaction rates calculated using the fourth-order kinetic equation were rejected by Zhang et al. (2000) based on natural analogue information, but the cited studies by Graf et al. (1961) and von der Borch (1965) do not appear to support this conclusion (see Section 4.1.3).

The magnesium ion must be dehydrated for the formation of magnesite to occur; this process could become progressively more difficult at lower temperatures, resulting in a higher activation energy barrier at lower temperatures. This effect could significantly decrease predicted lower-temperature reaction rates. However, Zhang et al. (2000) assumed that the activation energy remained constant when they extrapolated their rate constants to lower temperatures.

The experiments performed by Sayles and Fyfe (1973) and Zhang et al. (2000) provide qualitative indications of factors that could influence rates at lower temperature conditions. Sayles and Fyfe (1973) performed laboratory experiments at relatively low ionic strength and found that the formation of magnesite from hydromagnesite occurs more rapidly at high CO_2 pressure. The low CO_2 fugacities in the repository, therefore, may result in a relatively low rate of magnesite formation. Both Sayles and Fyfe (1973) and Zhang et al. (2000) demonstrated that higher magnesium concentrations slowed the rate at which hydromagnesite converted to magnesite. Consequently, the presence of magnesium in the WIPP brines after reaction with MgO, halite, and anhydrite (Brush et al. 2006) may result in a slower reaction rate. The presence of sulfate in WIPP brines may also decrease the hydromagnesite-to-magnesite conversion rate. However, Zhang et al. (2006) found that increasing ionic strength increased the conversion rate, so the high ionic strength of WIPP brines could increase the rate at which hydromagnesite converts to magnesite in the repository.

4.1.3 Natural Analogues

The occurrence of magnesite in low-temperature sediments is not always the result of dehydration of hydromagnesite, because magnesite appears to form directly from low-temperature solutions in a limited number of environments. Sayles and Fyfe (1973) noted that most modern low-temperature occurrences of magnesite are associated with solutions that have salinities greatly in excess of seawater, in which the lower activity of water favors dehydration of the magnesium ion. This association of magnesite with hypersalinity is consistent with its apparent direct precipitation in relatively recent deposits, including the Tuz Gölü seasonal salt lake in Turkey (Irion and Müller 1968), playa basins of the Cariboo Plateau of British Columbia (Renaut and Stead 1990), and a sabkha in Abu Dhabi (Evans et al. 1969). Based on these occurrences, direct precipitation of magnesite from solution appears to occur in highly saline conditions generated in seasonal salt lakes or mudflats that experience evaporation to dryness or near dryness.

Direct precipitation of magnesite at low temperatures appears to be favored by extremely high Mg/Ca ratios, with reported ratios up to 300 in Cariboo Plateau waters (Renaut and Stead 1990), and ratios of 85 to 149 in the porewaters and overlying brines of the Tuz Gölü salt lake (Irion and Müller 1968). In comparison, the Mg/Ca ratios in WIPP brines after reaction with MgO, halite, and anhydrite fall into a lower range; 14.7 for ERDA-6[4] and 64.6 for GWB. There also may be evidence that direct precipitation of magnesite is influenced by bacterial biomineralization (Thompson and Ferris 1990). Formation of magnesite directly through the carbonation of brucite formed from MgO is unlikely to occur in the WIPP repository, because laboratory experiments performed for the WIPP program have indicated that metastable hydromagnesite formation will precede magnesite formation under expected repository conditions (Bryan and Snider 2001a, Snider and Xiong 2002, Xiong and Snider 2003).

---

[4] The magnesium concentration in ERDA-6 brine was erroneously listed as 157 M in Table 3 of Brush et al. (2006). The correct concentration is 0.157 M. This typographical error did not affect any later calculations, such as the calculation of MgO lost with outflowing brine, because Clayton and Nemer (2006) used the correct magnesium concentration.

Natural analogues may provide evidence regarding the rate at which hydromagnesite will transform to magnesite. Although descriptions of natural occurrences of hydromagnesite can be found in the literature, most descriptions of these deposits do not establish the length of time it has persisted without converting to magnesite. For example, Brush and Roselle (2006) cited the occurrence of hydromagnesite as a weathering product of the New Idria serpentinite body to show that brucite will carbonate. However, they did not provide information regarding the length of time over which weathering and hydromagnesite formation had occurred. If the hydromagnesite in this deposit has persisted for thousands of years, it would indicate that hydromagnesite conversion to magnesite can be relatively slow in some environments.

Zhang et al. (2000) cited the occurrence of magnesite at Lake Bonneville and in southeastern Australia as evidence that hydromagnesite-to-magnesite conversion would be relatively rapid. Graf et al. (1961) described a mixture of fine-grained aragonite and a "magnesite-like material with a significantly expanded unit cell" in the sediments of Glacial Lake Bonneville on the Bonneville Salt Flats. The age of these sediments, determined using carbon-14 measurements, was established as $11,300 \pm 250$ years. The unit cell of the magnesite-like material was expanded relative to synthetic magnesite; this effect was attributed to residual water in the solid phase. Graf et al. (1961) stated that the hydrated magnesite may have formed by conversion of hydromagnesite that originally precipitated with the aragonite, or that the hydrated magnesite may have precipitated with aragonite. Thus, this "magnesite-like" material could have been directly precipitated and may not show that hydromagnesite will completely convert to magnesite within the 10,000-year WIPP regulatory period. The magnesite described in sediments from an ephemeral lake in southeastern Australia had an expanded unit cell similar to the material from Lake Bonneville (von der Borch 1965). The origin of the magnesite from the ephemeral lakes in southeastern Australia was unclear, and von der Borch (1965) stated that the magnesite may have either formed directly from solution or been transformed from hydromagnesite.

Stamatakis (1995) reported the occurrence of relatively thick hydromagnesite deposits (4 to 10 meters) in Neogene (< 23 million years) sediments. At the time of the CCA, EPA noted the apparent persistence of hydromagnesite in these sediments over potentially long periods of time, indicating that hydromagnesite conversion to magnesite could be relatively slow. Brush and Roselle (2006) stated that the deposit described by Stamatakis (1995) is irrelevant to WIPP, because the hydromagnesite was described as being of composition $Mg_4(CO_3)_3(OH)_2 \bullet 3H_2O(s)$, which differs from the composition of $Mg_5(CO_3)_4(OH)_2 \bullet 4H_2O(s)$ observed in WIPP experiments and used in WIPP geochemical calculations. However, as noted in Section 4.1 above, there is no evidence that the two reported formulas for hydromagnesite represent different phases. Brush and Roselle (2006) concluded that this evidence does not show that hydromagnesite has persisted longer than expected, based on the results of Zhang et al. (2000); on the other hand, Brush and Roselle (2006) did not provide any evidence that the hydromagnesite deposits described by Stamatakis (1995) are significantly less than 10,000 years old.

Evidence that hydromagnesite can persist for significant time periods is provided by Vance et al. (1992). This investigation describes the sediments associated with Chappice Lake, a saline lake in southwestern Alberta. The sediment core data span 7,300 years; the chronology of these sediments was determined from radiocarbon ages of seeds from upland plants and the presence

of plant pollen. The mineralogical data from the sediment cores indicate that hydromagnesite was present in sediments with ages up to approximately 6,200 years, with magnesite observed only in sediments in excess of 3,600 years in age. The presence of hydromagnesite below some magnesite in the core may indicate that the magnesite formed as a direct precipitate, rather than by conversion from hydromagnesite. The apparent persistence of hydromagnesite for as long as 6,200 years appears inconsistent with the extrapolated 25ºC rate data of Zhang et al. (2000).

4.1.4   Conclusions Regarding Conversion of Hydromagnesite to Magnesite

Based on the information reviewed above, there is significant uncertainty regarding the rate at which hydromagnesite can convert to magnesite, and whether all hydromagnesite will convert to magnesite during the WIPP regulatory time period. There are many uncertainties associated with the extrapolation of the Zhang et al. (2000) laboratory data to WIPP conditions, including the form of the rate equation, the effects of the hydromagnesite chemical and physical properties on the induction period, the uncertainties in determining the rates during the induction period, and whether the activation energy will remain constant at lower temperatures.

The available natural analogue data show that magnesite may form relatively quickly under some conditions, particularly in hypersaline environments with high Mg/Ca ratios. This information was considered during EPA's review of the CCA (EPA 1998c). However, DOE has not demonstrated that all hydromagnesite that forms under WIPP conditions will convert to magnesite within 10,000 years. In fact, information from one natural analogue indicates that hydromagnesite can persist for time periods on the order of 6,200 years. Such a slow rate of hydromagnesite to magnesite conversion in WIPP could result in the persistence of hydromagnesite throughout much, if not all, of the 10,000-year regulatory period. Because of the uncertainties associated with the rate at which hydromagnesite can convert to magnesite, it is more defensible to assume that the *r* parameter in equation (1) is equal to a range of 0.8 (hydromagnesite only) to 1.0 (magnesite only), with a uniform distribution across this range.

4.2   CALCITE AND PIRSSONITE PRECIPITATION

Microbial degradation of CPR is likely to proceed via the sulfate reduction reaction (7) after the limited amount of nitrate in the waste is consumed. Sulfate reduction could lead to dissolution of sulfate minerals in the Salado Formation, such as anhydrite, gypsum, and polyhalite, as sulfate solution concentrations decline. Dissolution of these sulfate minerals would release calcium ions, and increased calcium concentrations could result in calcite [$CaCO_3(s)$] and pirssonite [$Na_2Ca(CO_3)_2 \bullet 2H_2O$] precipitation and CO_2 consumption:

$$Ca^{2+} + CO_2 + H_2O \rightarrow CaCO_3(s) + 2\ H^+ \tag{15}$$

$$2\ Na^+ + Ca^{2+} + 2\ CO_2 + 4\ H_2O \rightarrow 2\ Na_2Ca(CO_3)_2 \bullet 2H_2O + 4\ H^+ \tag{16}$$
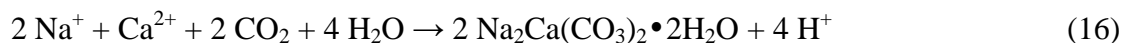
If significant precipitation of carbonate phases such as calcite or pirssonite occurs, it will increase CO_2 consumption per mole of MgO in the repository. Calcite precipitation generally occurs readily from oversaturated solutions at low temperatures, so calcite formation in the

repository is very likely. Brush et al. (2006) considered the potential effects of calcite and pirssonite precipitation on CO_2 consumption, and used these results to calculate y_{yield} values.

4.2.1 Geochemical Calculations

Brush et al. (2006) used the EQ3/6 geochemical software package to calculate the effects of sulfate mineral dissolution, sulfate reduction, and precipitation of calcite and pirssonite on y_{yield}. The EQ3/6 software package is well documented and widely used (Daveler and Wolery 1992, Wolery 1992a, Wolery 1992b, Wolery and Daveler 1992). Most of the thermodynamic data used in the calculations were from the EQ3/6 database provided with the software package, and may differ from the FMT thermodynamic databases reviewed by EPA during the CCA and CRA-2004.

The Pitzer EQ3/6 thermodynamic database used by Brush et al. (2006) did not include the sulfide species in reaction (7). In addition, the database did not include iron and silica species that could be important for buffering pH at higher pH values. Consequently, the reaction-path calculations performed by Brush et al. (2006) predicted pH values as high as 11.3 for many of the calculations. These extremely high pH values significantly exceeded previously predicted values (e.g., Brush 2005) and the Chemical Conditions conceptual model used in the WIPP PA (DOE 2004, Appendix PA Attachment SOTERM). Brush et al. (2006) attributed the high pH values to the inclusion of polyhalite in the Salado mineral assemblage. However, the high pH values predicted by the modeling calculations appear to be the result of the way in which the reactions were formulated in the EQ3/6 calculations. Brush et al. (2006) limited the amount of anhydrite to that necessary for CPR degradation by the denitrification reaction (6) and sulfate reduction reaction (7). In the EQ3/6 calculations that resulted in high pH values, all anhydrite was dissolved prior to the completion of the reaction path simulations. Consumption of all anhydrite in the modeled system is inconsistent with the Chemical Conditions conceptual model, which includes the assumption that WIPP brines remain in equilibrium with halite, anhydrite, and brucite (Wilson et al. 1996a). In addition, because of the lack of thermodynamic data for constituents such as ferrous iron [Fe^{2+}], sulfide [S^{2-}], bisulfide [HS^-], and hydrogen sulfide [$H_2S(aq)$], these potentially important species were not included in the modeled reactions.

Because of the limitations in the EQ3/6 database used by Brush et al. (2006), the geochemical modeling calculations that resulted in high predicted pH values are not representative of the WIPP repository chemistry. In addition, the assumption that all available anhydrite could be consumed is inconsistent with the peer-reviewed Chemical Conditions conceptual model. After consideration of EPA's comments on the EQ3/6 calculations and the database limitations, DOE requested that the Brush et al. (2006) evaluation should not be included in the technical basis for EPA's decision regarding the MgO Planned Change Request (Moody 2007). Because of the difficulties associated with quantifying the precipitation of calcite, Vugrin et al. (2007) assumed that y_{yield} was equal to 1 for the revised EEF calculations. This is a conservative and bounding assumption, because it is likely that calcite precipitation will occur in the repository if significant CO_2 is produced by microbial CPR degradation.

4.2.2 Effects of Limited Sulfate

The sequential use of electron acceptors from denitrification, then sulfate reduction, and finally methanogenesis has been assumed in evaluations of microbial gas generation in the WIPP repository. Consequently, if limited amounts of nitrate and sulfate are available for microbial respiration, significant amounts of CPR degradation could occur by the methanogenesis reactions (8) or (9). Significant methanogenesis would result in a lower y_{yield} value, because only half of the CPR carbon would be transformed into CO_2 via reaction (8), instead of the 1 mole of CO_2 per mole of CPR carbon produced in reactions (6) and (7). Methanogenesis by reaction (9) would result in an even lower y_{yield} value.

Whether nitrate and sulfate in the WIPP waste and intruding brines would be sufficient for microbial degradation of CPR only through denitrification and sulfate reduction can be determined by evaluating the amounts of nitrate and sulfate in these sources relative to the CPR carbon in the repository. WIPP waste is the only significant source of nitrate in the repository. The PABC inventory included 4.31×10^7 moles of nitrate (Leigh 2005). Because 0.8 moles of nitrate is consumed for each mole of CO_2 produced during denitrification, this amount of nitrate would result in the transformation of 4.5% of the carbon in the CPR into CO_2 via reaction (6). The estimated sulfate in the inventory was 4.61×10^6 moles (Leigh 2005). Because sulfate reduction produces 2 moles of CO_2 per mole of sulfate consumed, this amount of sulfate could react with 9.22×10^6 moles of CPR carbon, or 0.8% of the carbon in the inventory.

In addition to sulfate in the waste, sulfate will be present in the brine that enters the repository. Based on the PABC results, the maximum volume of brine expected to enter a panel is 13,267 m^3 of ERDA-6 brine (Clayton 2006). Because there are 10 panels in the repository, this volume would be 132,670 m^3 in the entire repository. The sulfate concentration in ERDA-6 brine is 0.170 mole/L, so the amount of sulfate in 132,670 m^3 of ERDA-6 brine is 2.26×10^7 moles. Reduction of this quantity of sulfate would consume an additional 3.7% of the CPR carbon in the inventory. In total, microbial consumption of the nitrate and sulfate in the waste and the maximum sulfate in the intruding brine would consume only about 9% of the CPR carbon in the repository. Consequently, sulfate reduction can be the dominant microbial degradation reaction only if significant quantities of sulfate are available from the dissolution of sulfate-bearing minerals in the Salado Formation.

EPA has previously considered the possibility that adequate amounts of sulfate may not be transported from the DRZ to CPR in the waste by reviewing the analysis presented in Kanney et al. (2004). This review was documented in TEA (2004). Whether methanogenesis will occur in the repository will depend on the relative rates of CPR degradation and transport of sulfate from dissolution of DRZ minerals to the waste. If the rate of sulfate transport by advection or diffusion is less than the rate of sulfate consumption, sulfate in the waste regions could become sufficiently depleted and methanogenesis could occur. Kanney et al. (2004) evaluated the possible diffusive transport of sulfate. Kanney et al. (2004) used the following equation to estimate the characteristic diffusion length:

$$L_{diff}^{SO4} = \sqrt{4 D_{eff}^{SO4} T_{bio}} \tag{17}$$

where:

L_{diff}^{SO4} = characteristic diffusion length for sulfate (m)

D_{eff}^{SO4} = effective sulfate diffusion coefficient (1.413×10^{-4} m²/yr)

T_{bio} = time period over which CPR degradation may occur (yr)

Using this equation, the characteristic diffusion length over 10,000 years is 2.38 m (7.80 ft). Consequently, sulfate from DRZ minerals present within 2.38 m of the repository walls could be transported to the waste by diffusion and be available for sulfate reduction. Based on information provided by Brush et al. (2006, Excel file calcite.xls), the thickness of the DRZ below the repository is 2.23 m, the DRZ thickness above the repository is 11.95 m, and the waste area is 1.12×10^5 m², which yields a total DRZ volume of 1.58×10^6 m³. The sulfate mineral content of the DRZ has been estimated, based on Brush's (1990) evaluation of data reported by Stein (1985). These data were obtained from two 50-foot cores drilled above and below Test Room 4, located near the repository horizon. This estimate, reported by Kanney et al. (2004) and Brush et al. (2006), was 93.2 wt % halite (NaCl) and 1.7 wt % each of magnesite, gypsum, anhydrite, and polyhalite. Using these percentages of the different minerals and the sulfate content of each mineral, Brush et al. (2006) calculated that the Salado Formation contains 3.23 wt % sulfate. The amount of sulfate required from the DRZ minerals for sulfate reduction to take place after sulfate in the waste has been consumed is 5.68×10^8 moles. This represents 49% of the total estimated amount of sulfate in the DRZ minerals.[5]

The amount of sulfate contained in DRZ minerals within the 2.38 m diffusion distance can be determined using the average Salado sulfate content of Brush (1990). The results of this calculation indicate that within the 2.23 m thick DRZ below the repository and the 2.38 m DRZ above the repository, 66% of the required sulfate is available for consumption of CPR carbon by sulfate reduction. However, use of the average sulfate content in the two 50-foot sections reported by Stein (1985) does not take into account the heterogeneous distribution of sulfates in the Salado Formation. Currently, disposal rooms are excavated up to Clay Seam G, and the Anhydrite B layer is removed to improve roof stability. Examination of the lithologic logs in Stein (1985, Appendix A) indicates that the Anhydrite A layer is located within approximately 2 meters of the top of the disposal rooms; the Anhydrite B material at the sides of the repository would also be available for sulfate dissolution and transport into the disposal rooms. The halite layer between the top of the disposal rooms and Anhydrite A contains anhydrite stringers and laminae. These anhydrite inclusions have been visually observed in the walls and roof of the disposal rooms and were noted in the cores by Stein (1985). Consequently, it appears that the sulfate content of the Salado Formation closest to the repository could be higher than the average values calculated by Brush (1990), and sufficient sulfate may be available for CPR degradation by sulfate reduction. The possible advective transport of sulfate and the effects of sulfate coming into direct contact with waste due to disposal room collapse may also increase the availability of sulfate.

---

[5] Brush et al. (2006) calculated that the amount of sulfate required was 44% of the sulfate in the DRZ; however, this number was corrected in the present report to account for the additional CPR carbon in emplacement cellulosics and plastics.

The results of the TEA (2004) review indicated that DOE had not conclusively demonstrated that sulfate in the DRZ will be unavailable for sulfate reduction. It was pointed out that DOE assumed a 2,000-year time period for diffusion instead of 10,000 years (Kanney et al. 2004). This limited time period has since become more significant, because of the use of lower long-term CPR degradation rates in the PABC than in the PAVT. In addition, TEA (2004) found that DOE had not adequately accounted for potential structural failure, such as a roof collapse that could bring sulfate-bearing minerals into direct contact with repository brine or even settling of the roof directly onto the waste stacks. DOE has not provided any additional information since the analysis of Kanney et al. (2004). Consequently, it is still appropriate to conservatively assume that all carbon in CPR could be completely converted to CO_2, and that no methanogenesis will occur for the purposes of calculating required amounts of MgO in the backfill.

However, it should be recognized that assuming that all CPR carbon will be completely converted to CO_2 is a bounding assumption. Although there may be sufficient sulfate in the Salado Formation minerals to prevent widespread methanogenesis, heterogeneous waste emplacement or heterogeneity in the mineralogy of the Salado Formation could lead to limited methanogenesis, even if the overall rate of sulfate transport is relatively high. Any methanogenesis that occurs would reduce y_{yield} and increase the EEF.

4.2.3 Potential Effects of Inhibitors

Although geochemical modeling calculations have not been carried out to quantify the effect of calcium-carbonate precipitation on y_{yield}, precipitation of a calcium-carbonate solid is likely to occur in the repository if significant CO_2 is produced by CPR degradation. Precipitation of a calcium-carbonate solid is particularly likely if a significant amount of microbial sulfate reduction occurs and sulfate concentrations decrease. Decreased sulfate concentrations would result in anhydrite or gypsum dissolution; dissolution of these phases would result in increased dissolved calcium concentrations that would promote calcium carbonate precipitation. Precipitation of a calcium-carbonate phase would consume CO_2 and cause y_{yield} to be less than 1.

A number of constituents present in the WIPP waste and brines are known to inhibit the formation of various calcium-carbonate phases. As summarized by Brush et al. (2006), these potential inhibitors include magnesium, phosphate, sulfate, iron, citrate, EDTA, oxalate, and humic acid. Brush et al. (2006) evaluated the available information related to calcium carbonate inhibition to determine if any of these inhibitors could prevent calcium carbonate precipitation. The results of their review indicated that individual inhibitors, such as magnesium ion, could prevent the formation of calcite, which is the most thermodynamically stable calcium-carbonate phase. However, when calcite formation is inhibited, other calcium-carbonate phases that are more soluble, such as aragonite, vaterite, and amorphous $CaCO_3(s)$, have been precipitated in many experiments.

A large number of calcite inhibition studies have been reported in the literature. Many of these studies focused on relatively short-term effects related to systems such as water processing equipment and cooling towers. Because of the abundant potential nucleation sites in the repository and the 10,000-year regulatory period, it is unlikely that any inhibitor or combination

of inhibitors would completely prevent nucleation and growth of a calcium-carbonate solid phase. Brush et al. (2006) identified aragonite and magnesium calcite ($Ca_{0.78}Mg_{0.22}CO_3$) as the calcium-carbonate phases most likely to form in the repository, based on the predicted concentrations of magnesium and citrate in repository brines and experimental data reported by Meldrum and Hyde (2001).

4.3   FORMATION OF OTHER CARBONATE PHASES

Brush and Roselle (2006) included weathered serpentinite bodies as natural analogues for the discussion of brucite carbonation. Brush and Roselle (2006) noted that in addition to hydromagnesite formation in parts of the weathered serpentinite bodies, pyroaurite [$Mg_6Fe_2(CO_3)(OH)_{16} \bullet 4H_2O$] and coalingite [$Mg_{10}Fe_2(CO_3)(OH)_{24} \bullet 2H_2O$] were observed as weathering products. These phases incorporate CO_2 in much lower proportions to magnesium than either magnesite or hydromagnesite. If coalingite or pyroaurite formed in the repository because of the presence of iron, this could significantly reduce the value of the *r* parameter in equation (1). These phases incorporate iron in the +III oxidation state. Because of the presence of iron metal and CPR degradation reactions, reducing conditions are expected to prevail in the repository, and iron is likely to be present in solution only in the +II oxidation state. Consequently, pyroaurite and coalingite are unlikely to form in the repository.

Iron and lead in the repository may consume microbially produced CO_2 and H_2S through the precipitation of iron-carbonate, lead-carbonate, iron-sulfide, and lead-sulfide phases. Formation of significant quantities of iron- or lead-carbonate phases could decrease the amounts of CO_2 available to react with the MgO backfill; however, the stability of iron- and lead-carbonate phases under WIPP conditions is unknown. In addition, the rates of formation of these phases have not been determined under anticipated WIPP conditions, and the possibility of passivation of the steel or lead surfaces cannot be completely ruled out (Brush and Roselle 2006). DOE has proposed experimental investigations to determine the stability and rates of formation of iron- and lead-carbonate and iron- and lead-sulfide phases under repository conditions (Wall and Enos 2006). Pending the results of these investigations, the potential effects of iron- and lead-carbonate phase precipitation were not included in the determination of y_{yield} values.

WIPP waste can contain no more than 1% free liquid on a volume basis, so WIPP waste generators use Portland cement to solidify waste sludges and liquids before shipment. Reaction of Portland cement results in the partial hydration of lime [CaO] in the cement to portlandite [$Ca(OH)_2$]. These phases can carbonate and consume CO_2. Brush and Roselle (2006) estimated 1.9×10^6 moles of lime would be available to react with CO_2, based on (1) an estimated amount of free lime (unreacted to form silicates) in Portland cements, (2) the mass of cement in the WIPP waste inventory, and (3) the molecular weight of lime. Brush and Roselle determined that reaction of this amount of lime to form calcite could consume 0.177% of the CO_2 produced by complete microbial consumption of all CPR materials in the repository. The effect of lime in Portland cement was not included in the evaluation of the EEF because of its relatively small magnitude.

4.4   CONSUMPTION OF CARBON DIOXIDE BY OTHER PROCESSES

Other processes that could limit the amount of CO_2 available for reaction with MgO include dissolution of CO_2 in brine and incorporation of carbon in biomass. Vugrin et al. (2006) did not include the potential effects of CO_2 dissolution in WIPP brines in their calculations of the EEF, based on the results of an analysis by Brush and Roselle (2006). Brush and Roselle (2006) determined that the amount of CO_2 likely to be dissolved in brine would be insignificant, because of the low total dissolved carbon predicted for GWB and ERDA-6 brines for the PABC and the relatively small volumes of brine likely to flow through the repository.

Biomass carbon would include carbon incorporated in microbial cells. The amount of CPR carbon that could remain sequestered in the biomass is uncertain. Sources of this uncertainty include the amounts of cellular material likely to be present in the repository, and whether other microbes could consume dead or dormant microbes. Because of the uncertainties associated with the amount of carbon that could remain in the biomass, the effects were not considered in the calculations. The effects of neglecting carbon in the biomass are likely to be at least slightly conservative.

4.5   CALCULATION OF CARBON DIOXIDE YIELD

Vugrin et al. (2006, 2007) defined y_{yield} as the moles of CO_2 produced per mole of consumed CPR carbon. Vugrin et al. (2006) included the effects of calcite precipitation in their determination of y_{yield}. However, because the EQ3/6 calculations used to predict the amount of calcite precipitation were found to be unrepresentative of the repository chemistry, Vugrin et al. (2007) did not include the effect of calcite precipitation on y_{yield} and assumed a value of 1 for this parameter. This is a conservative, bounding assumption, because it is likely that calcite precipitation and methanogenesis will occur in the repository, although the relative extents of these processes have not been quantified at this time.

5.0   EFFECTIVE EXCESS FACTOR CALCULATIONS

The EEF calculation is affected by uncertainties associated with CO_2 production, the availability of MgO for reaction with CO_2, and the moles of CO_2 consumed per mole of available MgO. The equation used by Vugrin et al. (2006, 2007) to represent these uncertainties can be modified to incorporate the uncertainty associated with chemical composition of the CPR:

$$EEF = \frac{(y_{SS} \times y_{RC} \times 0.999 - y_{L2B}) \times M_{MgO}}{(y_{yield} \times y_{CPR} \times y_{CPR-C}) \times M_C} \times r \qquad (18)$$

The values used by Vugrin et al. (2007) for these variables are summarized in Table 5, along with the revised values determined during this review. The only significant revision to the formulation of Vugrin et al. (2007) is the addition of the y_{CPR-C} uncertainty parameter; this parameter accounts for uncertainty in the CPR chemical composition.

Substituting the mean values in Table 5 into (18) results in the following:

$$EEF = \frac{(1 \times 0.96 \times 0.999 - 0.007) \times 1.44 \times 10^9}{(1 \times 1 \times 1.03) \times 1.2 \times 10^9} \times 0.9 = 1.00 \qquad (19)$$

The result of this calculation indicates that the average EEF equals the value needed to ensure that an adequate amount of MgO is emplaced in the repository. Vugrin et al. (2007) calculated σ_{EEF} equal to 0.0719. Because of the effect of uncertainty related to the CPR chemical composition, σ_{EEF} was recalculated and found to equal 0.0775. Given the uncertainty associated with the EEF, it might appear that it would be possible that an inadequate amount of MgO would be present in some repository disposal rooms. However, a number of significant, conservative assumptions were included in this calculation of the average EEF:

- No calcite will precipitate as a result of DRZ sulfate mineral dissolution

- No methanogenesis will occur, and every mole of CPR carbon that is microbially degraded will form CO_2

- All CPR carbon will be degraded

- No other carbonate minerals will form in the repository, including iron-carbonates, lead-carbonates, or calcite from lime and portlandite in cements

Table 5.   Variables and Parameters used in Effective Excess Factor Calculation

Variable	Description	Vugrin et al. (2007)	Comments
y_{ss}	Uncertainty in amount of CPR in a room relative to the amount tracked by DOE	$\mu_{SS} = 1.00$ $\sigma_{SS} = 3.7 \times 10^{-4}$	
y_{RC}	Concentration of reactive constituents in MgO	$\mu_{RC} = 0.96$ $\sigma_{RC} = 0.02$	This value is based on analysis of a single shipment. It appears that current acceptance criteria may not identify MgO with unacceptably low reactivity. However, the high chemical purity and consistency of the WTS-60 feedstock and production process indicates that WTS-60 MgO is likely to maintain this level of reactivity.
y_{L2B}	Loss of MgO to brine	$\mu_{L2B} = 0.007$ $\sigma_{L2B} = 0.017$	
0.999	Fraction of MgO that will remain uncarbonated after emplacement	0.999	
M_{MgO}	Total moles of emplaced MgO	$1.20 \times M_C$	
y_{yield}	Effective CO_2 yield (moles CO_2 per mole of consumed CPR carbon)	1.0	The CO_2 yield has been assumed equal to 1.0, because of difficulties associated with quantifying the effects of precipitation of calcite or other carbonate phases besides hydromagnesite or magnesite. If significant sulfate reduction occurs, however, calcite precipitation is likely, and this parameter will be less than 1.0. Alternatively, if insufficient sulfate is available, methanogenesis will be likely and this parameter will be less than 1.0.
y_{CPR}	Uncertainty in CPR mass estimates	$\mu_{CPR} = 1.00$ $\sigma_{CPR} = 3 \times 10^{-3}$	
y_{CPR-C}	Uncertainty in CPR carbon estimates – multiplier for estimated CPR carbon moles estimated using assumptions of Wang and Brush (1996)	$\mu_{CPR-C} = 1.03$ $\sigma_{CPR-C} = 0.03464$	Uniform distribution from 0.97 (reasonable low-range estimate) to 1.09 (reasonable upper-range estimate. This uncertainty parameter was introduced to account for potential variations in the chemical composition (moles carbon/kg) of the CPR.
M_C	Reported inventory of CPR carbon	1.21×10^9 moles	Calculated using CPR chemical composition assumptions of Wang and Brush (1996)
r	Moles CO_2 consumed per mole of MgO reacted	$\mu_r = 0.9$ $\sigma_r = 0.0577$	Uniform distribution from 0.8 (hydromagnesite) to 1.0 (magnesite). This parameter incorporates the uncertainty in the rate of hydromagnesite to magnesite conversion.

There is considerable uncertainty associated with the assumption that all CPR will be microbially degraded. A recent review of this issue indicated that microbial degradation of cellulosics in the repository is reasonably likely if brine is present (SCA 2006a). However, it is less certain that plastics and rubber will fully degrade during the 10,000-year regulatory period. Short-term data for plastics such as polyethylene and PVC, the two most abundant plastics in the WIPP inventory, indicate that these materials may not be readily degraded. However, there is considerable uncertainty regarding the long-term degradability of plastics and rubber because of the potential effects of radiolysis and the possible adaptability of microbes over the 10,000-year regulatory time period. Because the uncertainties associated with the long-term degradation of CPR materials cannot be quantified at this time, a conservative, bounding assumption has been made that all CPR carbon will be microbially degraded. The effect of this assumption is likely to be significant. To illustrate the possible magnitude of the conservatism associated with this assumption, the mean EEF was recalculated assuming that none of the plastics and rubber would degrade to form CO_2. The mean EEF calculated using this assumption was equal to 3.0. Thus, if plastics and rubber do not degrade to form CO_2, an EF of 1.20 in the repository would result in a threefold excess of MgO.

Another conservative, bounding assumption is that all CPR degradation will take place through denitrification and sulfate reduction, producing only CO_2 instead of a mixture of CO_2 and methane that would be produced by methanogenesis. Based on diffusion calculations and the amounts of sulfate minerals in the DRZ, it may be possible for sulfate to be transported to the waste in sufficient quantities to prevent widespread methanogenesis. However, methanogenesis may occur in waste areas where relatively rapid microbial degradation of CPR occurs or where the adjacent Salado Formation has relatively low sulfate mineral concentrations.

The formation of carbonates other than hydromagnesite or magnesite, particularly a calcium-carbonate phase such as calcite, is very likely. The effects of calcium-carbonate mineral formation on y_{yield} were not included in the uncertainty analysis because of difficulties encountered by DOE in their effort to quantify the amount of calcium-carbonate mineral precipitation that could occur. Significant quantities of DRZ sulfate minerals such as anhydrite or gypsum must dissolve and release calcium ions to the brine for CPR degradation to occur only through denitrification and sulfate reduction. Dissolution of these sulfate minerals would generate large quantities of calcium ions that will result in calcium-carbonate precipitation and an increase in the EEF. Because the effects of calcium-carbonate mineral precipitation were not included in this EEF uncertainty calculation, the results of this calculation are very conservative.

6.0   CHEMICAL CONDITIONS CONCEPTUAL MODEL

The repository geochemistry and solubility of actinides in brine can be affected by CPR degradation reactions, corrosion of metallic waste, brine compositions, and the mineralogy of the Salado Formation. The original Chemical Conditions conceptual model was described in CCA Appendix SOTERM (DOE 1996) and by the Conceptual Models Peer Review Panel (Wilson et al. 1996a). Key features of the CCA Chemical Conditions conceptual model are as follows:

- The Salado Formation is predominantly halite, with accessory anhydrite, gypsum, polyhalite, and magnesite. Small quantities of intergranular and intragranular brines are associated with the salt at the repository horizon. These brines are highly concentrated (up to 8 molar), with a composition of mostly sodium, magnesium, potassium, chloride, and sulfate, with smaller amounts of calcium, carbonate, and borate.

- The underlying Castile Formation is composed of bedded anhydrite and contains localized brine reservoirs under sufficient pressure to force brine upward to the land surface if penetrated by a borehole. Castile brines are concentrated solutions containing predominantly sodium chloride with calcium and sulfate, and smaller concentrations of other elements.

- Brine that dissolves actinides under any intrusion scenario will have a composition equal to that of Salado brine, Castile brine, or a mixture of Salado and Castile brines. Because the Salado and Castile brines bracket the possible brine compositions, experiments and modeling performed only with end-member brine compositions are adequate for describing the geochemistry of the repository. At the time of the CCA, Brine A was used to simulate Salado brines and ERDA-6 brine was used to simulate Castile brines.

- Equilibrium is assumed between repository brine and the Salado minerals halite, anhydrite, brucite, and magnesite. Polyhalite is not included explicitly in this equilibrium assumption, and it is not included in geochemical modeling calculations of actinide solubilities.

- Brine in the repository will be well mixed with waste.

- There is a 50% probability of no significant microbial degradation of CPR, a 25% probability that only cellulosics will degrade, and a 25% probability that cellulosics, plastics, and rubber will degrade.

- CPR degradation can occur by denitrification, sulfate reduction, and methanogenesis. Because of the limited amounts of nitrate and sulfate in the waste, methanogenesis is expected to be the primary CPR degradation reaction. A relatively large excess of MgO will be emplaced with the waste, with 1.95 moles of MgO per mole of CPR carbon. Consequently, the identity of the dominant CPR degradation reaction and the resulting proportions of CO_2 or methane produced (i.e., sulfate reduction or methanogenesis) will not affect repository performance because of the large excess of MgO.

- In the absence of MgO backfill, low pmH ($-\log_{10}$ of the hydrogen ion molality) and high CO_2 fugacity could be achieved in the repository brine, increasing the solubilities of actinides relative to neutral or slightly basic pmH and low CO_2 fugacity conditions. However, conditions that might lead to high actinide solubilities should not occur in the

repository because excess MgO emplaced as an engineered barrier will buffer the pmH and CO_2 fugacities of the brine to values where the actinide solubilities are minimized.

- Hydrated MgO will react with CO_2 to form magnesite. Cementitious material will contain $Ca(OH)_2$ that could also react with CO_2 to form calcite. This latter reaction could buffer pmH at relatively high values. However, the effect of $Ca(OH)_2$ is expected to be minimal because of calcite precipitation and reaction of the $Ca(OH)_2$ with $MgCl_2$ in the brine to form $CaCl_2$.

- Carbon dioxide fugacities that will prevail in the repository can be modeled using the brucite-magnesite buffer.

- Microbial degradation of CPR and/or steel corrosion will result in a reducing environment within 100 years of repository closure.

- Oxidation-reduction equilibrium with waste materials (including iron metal and CPR) is not assumed. Steel corrosion and CPR degradation are represented by reaction rates instead of equilibrium.

- Steel in the repository will corrode and reduce the oxidation states of some actinides, affecting their solubilities and binding constants.

- At low temperatures, a system-wide Eh is not always useful for describing oxidation-reduction conditions because of possible disequilibrium between various oxidation-reduction couples. Consequently, the expected oxidation states of the actinides are determined based on experimental data. Americium is assumed to occur in the +III oxidation state, thorium in the +IV oxidation state, plutonium in the +III or +IV oxidation state, neptunium in the +IV or +V oxidation state, and uranium in the +IV or +VI oxidation state.

- Although it is possible that microbial consumption of organic ligands in the waste could occur, because of uncertainty about the presence or viability of these types of microbes, it is assumed that organic ligand concentrations will not be reduced by microbial degradation.

- Steel corrosion will release iron and nickel ions into solution. These metal ions will bind with organic ligands and limit the ability of organic ligands to increase actinide solubility.

- High pressure in the repository is not expected to significantly affect actinide solubilities, so its effect is not considered in the geochemical calculations. Temperature in the repository is not expected to vary significantly from ambient, so temperature effects on solubility also are not considered.

- Brine radiolysis could produce reactive species, such as peroxide (H_2O_2). Any oxidized species such as peroxide are expected to react quickly with iron metal and dissolved iron(II) species in solution. Consequently, radiolysis is not expected to affect the oxidation-reduction conditions in the repository.

EPA reviewed the CCA conceptual model, and the only significant change was to the reaction expected to buffer CO_2 fugacity for the purpose of calculating actinide solubilities. Because of the potentially slow rate of conversion of hydromagnesite to magnesite, EPA required the

assumption that the brucite-hydromagnesite reaction would buffer CO_2 fugacities at higher levels than the brucite-magnesite buffer. The potential occurrence of methanogenesis was not considered important, because of the large excess of MgO in the backfill.

DOE (2004) made some changes to the Chemical Conditions conceptual model for the CRA-2004:

- A minor change was made to the simulated Salado brine composition, from Brine A to GWB, because GWB was believed to better represent the composition of intergranular brines. The effects of this change in brine composition on actinide solubilities were reviewed and found to be negligibly small (EPA 2006b).

- Because of the availability of thermodynamic data for the organic ligands, the interaction of the actinides and ligands were modeled using FMT and the newly available thermodynamic data. DOE stated that the solubilities of the +III and +IV actinides would not be significantly affected by acetate, citrate, oxalate, or EDTA complexation.

EPA (2006b) reviewed the CRA-2004 information, and on the basis of this review and additional data developed since the PAVT, required the following changes to the Chemical Conditions conceptual model for the PABC:

- Microbial degradation experiments carried out for the WIPP program indicated that microbial degradation of cellulosics was more likely because of the presence of microbes in WIPP that were capable of effectively degrading cellulosics. These data also indicated that the long-term rates of CPR degradation were likely to be significantly lower than the rates used in the CCA PA, the PAVT, and the CRA-2004 PA. Therefore, the probability of cellulose degradation was increased to 100%, and lower long-term degradation rates were used to model gas generation.

- The results of geochemical modeling indicated that the solubilities of the +III and +V actinides were increased by EDTA and oxalate complexation, respectively.

- Because of information developed during the review of the AMWTP (TEA 2004), EPA believed that sulfate dissolved in brine and the dissolution of DRZ minerals such as anhydrite and gypsum could cause sulfate reduction to be the dominant CPR degradation reaction. As a result, the occurrence of significant amounts of methanogenesis should not be assumed for the purposes of calculating the required amounts of MgO in the repository backfill.

Since the time of the CCA, the WIPP Chemical Conditions conceptual model has been updated as additional data became available. These changes to the Chemical Conditions conceptual model have been relatively minor. At this time, the current Chemical Conditions conceptual model appears to be consistent with the available data, and the model appears to adequately represent expected conditions in the repository.

7.0   CONCLUSIONS

Vugrin et al. (2006) summarized the uncertainty analysis associated with the amount of MgO required to react with CO_2 and control chemical conditions in the WIPP repository. This summary and the characterization of the uncertainties and their effects on the EEF calculations provided a reasonable approach for addressing these uncertainties. However, a review of Vugrin et al. (2006) and the supporting information indicated that some uncertainties were not adequately considered. DOE provided a revised evaluation of the uncertainties based on comments from EPA and additional analysis (Vugrin et al. 2007).

Uncertainties associated with the required amount of MgO backfill were divided into four general categories (Vugrin et al. 2006, 2007). These uncertainties were the amount of CPR carbon that would be consumed, the quantities of CO_2 that would be produced by CPR degradation, the amount of MgO that would be available to react with the CO_2, and the moles of CO_2 that would react per mole of MgO. Characterization of the latter uncertainty included the possible formation of carbonate phases other than magnesium carbonates.

The amount of CPR carbon that will be consumed in the WIPP repository will depend on the total available amount of CPR carbon and the likelihood of its microbial degradation during the repository regulatory period. Vugrin et al. (2007) adequately characterized the uncertainty associated with the mass of CPR in the WIPP inventory, based on a statistical analysis by Kirchner and Vugrin (2006). However, the molar quantity of CPR carbon calculated from this CPR mass inventory was based on assumptions about the chemical composition of the CPR. The uncertainty related to the CPR chemical composition appears to have a relatively small effect on the EEF uncertainty. There is considerable uncertainty associated with the long-term microbial degradation rates of plastics and rubber in the repository environment. This uncertainty was addressed by making the bounding and conservative assumption that all available CPR materials would be microbially degraded.

The quantities of CO_2 that could be produced by CPR degradation will depend on the microbial respiration reactions. Because of the abundant sulfate minerals in the Salado Formation, it was assumed that all CPR degradation would occur by denitrification or sulfate reduction, and one mole of CO_2 would be produced for each mole of CPR carbon consumed. This is a bounding and conservative assumption, because if any CPR degradation occurs via methanogenesis, the ratio of CO_2 produced per mole of CPR carbon consumed will be smaller.

Uncertainties related to the amount of MgO available to react with CO_2 include the mass of MgO per supersack, the amount of MgO that could carbonate before emplacement, and the amount of MgO dissolved in brine that could flow out of the repository during a human intrusion event. These uncertainties were adequately incorporated in the EEF calculations based on an analysis of the available data. Magnesium in inflowing Salado brine could carbonate and remove a relatively small fraction of the CO_2 from solution; this process was evaluated and conservatively omitted from the uncertainty calculations. The potential for MgO segregation from brine and CO_2 was not found to be a likely source of uncertainty, because it is very likely that the MgO supersacks will rupture and it is very unlikely MgO will be physically segregated by room roof collapse. The Conceptual Models Peer Review Panel (Wilson et al. 1997b) and EPA (1997)

considered the available data regarding the possible formation of reaction rims on periclase grains or impermeable reaction layers on larger masses of MgO to determine whether such reaction rims or layers could make a significant amount of the MgO unavailable for reaction. Based on a consideration of these data, both the Conceptual Models Peer Review Panel and EPA (1997) concluded that essentially all MgO would remain available for reaction with brine and CO_2. However, both the Conceptual Models Peer Review Panel (Wilson et al. 1997b) and EPA (1997) cited the large excess of MgO in the backfill during their consideration of the ability of the MgO backfill to control chemical conditions in the repository. Diffusion calculations have indicated that mixing caused by aqueous diffusion will be sufficient to maintain a well-mixed repository and permit contact and reaction of MgO, brine, and CO_2. Advection and dispersion processes, which were not accounted for in the calculations, are likely to provide an even greater level of mixing.

The reactive fraction of MgO in the repository backfill was quantified by analyzing samples from one shipment of the WTS-60 MgO supplied by Martin Marietta; the results indicated the reactive fraction was 96 ± 2 mole %. This mean reactive fraction and uncertainty were used to calculate the EEF. Information on the manufacturing process and feedstock materials for the WTS-60 MgO indicates that the chemical variability of different shipments of this material will be low, and it appears likely that the WTS-60 MgO will consistently contain this fraction of reactive material. The hydration and carbonation experiments proposed by Deng et al. (2006b) would help confirm that different shipments of the WTS-60 MgO have the required fraction of reactive material, and that this material will carbonate at a rate that is sufficient to control CO_2 partial pressures in the repository.

The moles of CO_2 consumed per mole of reacted MgO will depend on the carbonate phases that form in the repository. Magnesite is the stable magnesium carbonate phase under repository conditions, but metastable hydromagnesite is expected to form initially and may persist throughout much, if not all, of the repository regulatory period. Because of the uncertainties associated with the hydromagnesite-to-magnesite conversion rate, the ratio of the moles of CO_2 consumed per mole of MgO was parameterized as a uniform distribution from 0.8 to 1.

If a significant amount of CPR degradation takes place via sulfate reduction, dissolution of Salado sulfate minerals such as anhydrite and gypsum will release calcium ions to solution. The increased calcium concentration should result in the precipitation of a calcium-carbonate phase, such as calcite, which would increase the moles of CO_2 consumed per mole of MgO reacted. However, because of difficulties in quantifying calcium carbonate precipitation, the conservative and bounding assumption was made that no calcium carbonate precipitation would occur. On the other hand, if insufficient nitrate or sulfate is available, CPR degradation is likely to proceed by methanogenesis, rather than denitrification or sulfate reduction. Either calcium carbonate precipitation or methanogenesis would reduce the quantity of MgO required to control CO_2 fugacities in the repository. The effects of CO_2 dissolution in brine are likely to be small, and were neglected in the calculation of the amount of CO_2 consumed per mole of MgO; the incorporation of carbon in biomass conservatively was not considered in the EEF calculation because of uncertainty regarding this process.

Because of revisions to the parameters describing the moles of CO_2 consumed per mole of reacted MgO and to the CO_2 yield per mole of degraded CPR carbon, plus a small increase in the CPR carbon inventory estimates because of emplacement cellulosics and plastics, the average EEF of 1.60 calculated by Vugrin et al. (2006) was reduced to 1.03 in the evaluation by Vugrin et al. (2007). Incorporating the uncertainty associated with the chemical composition of CPR materials in WIPP inventory ultimately reduced the average EEF to 1.00; however, this calculation of the EEF includes a number of conservative assumptions, as noted above. The most important conservative assumptions are that all CPR carbon will degrade, no methanogenesis will occur, and no precipitation of a calcium-carbonate solid phase will take place. Given these conservative, bounding assumptions, it is likely that the EEF will be greater than the average calculated value of 1.00, and an excess of MgO will be present if the EF is 1.20. Consequently, reducing the EF from 1.67 to 1.20 is unlikely to significantly affect WIPP repository chemistry, based on the available information.

During their respective reviews of the Chemical Conditions conceptual model and the effectiveness of the MgO engineered barrier at the time of the CCA and the CCA PAVT, both the Conceptual Models Peer Review Panel (Wilson et al. 1997b) and EPA (1997) took into account the presence of a large excess of MgO relative to the amount of CPR carbon in the repository when considering the reactivity of the MgO engineered barrier. The extent to which the conservative assumptions used to calculate the average EEF of 1.00 provide an adequate margin that offsets the reduced excess MgO is somewhat uncertain. Although the effects of these conservative assumptions have not been quantified, they are potentially significant: an example calculation indicates that up to a threefold excess of MgO over the amount required would be present if the EF was 1.20 and no plastics and rubber degraded to form CO_2.

The Chemical Conditions conceptual model has evolved since the CCA because of the availability of additional information about processes, such as microbial degradation and complexation of actinides by organic ligands. The changes to the Chemical Conditions conceptual model from the time of the CCA PA to the present have been relatively minor, and the current Chemical Conditions conceptual model remains consistent with expected repository conditions.

8.0   REFERENCES

Brush, L.H., 1990. *Test Plan for Laboratory and Modeling Studies of Repository and Radionuclide Chemistry for the Waste isolation Pilot Plant.* SAND90-0266, Sandia National Laboratories, Albuquerque, New Mexico.

Brush, L.H., 1995. *Systems Prioritization Method – Iteration 2 Baseline Position Paper: Gas Generation in the Waste Isolation Pilot Plant.* Unpublished report, Sandia National Laboratories, Albuquerque, New Mexico, March 17, 1995. ERMS 228740.

Brush, L.H., 2004. *Implications of New (Post-CCA) Information for the Probability of Significant Microbial Activity in the WIPP.* Sandia National Laboratories Carlsbad Programs Group, Carlsbad, New Mexico, July 28, 2004. ERMS 536205.

Brush, L.H., 2005. *Results of Calculations of Actinide Solubilities for the WIPP Performance-Assessment Baseline Calculations.* Sandia National Laboratories, Carlsbad, New Mexico. ERMS 539800.

Brush, L.H. and G.T. Roselle, 2006. Geochemical Information for Calculation of the MgO Effective Excess Factor. Memorandum to E.D. Vugrin, Sandia National Laboratories, Carlsbad, New Mexico, November 17, 2006.

Brush, L.H., Y. Xiong, J.W. Garner, A. Ismail, and G.T. Roselle, 2006. *Consumption of Carbon Dioxide by Precipitation of Carbonate Minerals Resulting from Dissolution of Sulfate Minerals in the Salado Formation in Response to Microbial Sulfate Reduction in the WIPP.* Sandia National Laboratories, Carlsbad, New Mexico.

Bryan, C.R., and A.C. Snider, 2001a. MgO Experimental Work Conducted at SNL/CB: Continuing Investigations with Premier Chemicals MgO, *Sandia National Laboratories Technical Baseline Reports, WBS 1.3.5.4, Repository Investigations, Milestone RI020, July 31, 2001.* Sandia National Laboratories, Carlsbad, New Mexico. ERMS 518970, pp. 5–1 to 5–15.

Bryan, C.R., and A.C. Snider, 2001b. MgO Hydration and Carbonation at SNL/Carlsbad, *Sandia National Laboratories Technical Baseline Reports, WBS 1.3.5.4, Repository Investigations, Milestone RI010, January 31, 2001.* Sandia National Laboratories, Carlsbad, New Mexico. ERMS 516749, pp. 66–83.

Bynum, R.V., C. Stockman, Y. Wang, A. Peterson, J. Krumhansl, J. Nowak, J. Cotton, S.J. Patchet, and M.S.Y. Chu, 1996. *Implementation of Chemical Controls through a Backfill System for the Waste Isolation Pilot Plant (WIPP).* SAND-96-2656C, Sandia National Laboratories, Albuquerque, New Mexico.

Chapelle, F.H., 1993. *Ground-Water Microbiology & Geochemistry.* John Wiley & Sons, New York.

Christ, C.L., and P.B. Hostetler, 1970. Studies in the system $MgO-SiO_2-CO_2-H_2O$ (II): the activity product constant of magnesite. *American Journal of Science* 268:439–453.

Clayton, D., 2006. *Update of the Minimum Brine Volume for a Direct Brine Release and New Maximum Castile and Salado Brine Volumes in a Waste Panel*. Memorandum to L.H. Brush, Sandia National Laboratories, Carlsbad, New Mexico, October 11, 2006. ERMS 544453.

Clayton, D. and M. Nemer, 2006. *Normalized Moles of Castile Sulfate Entering the Repository and Fraction of MgO Lost Due to Brine Flow Out of the Repository*. Memorandum to E.D. Vugrin, Sandia National Laboratories, Carlsbad, New Mexico, October 9, 2006.

Daveler, S.A., and T.J. Wolery, 1992. *EQPT, A Data File Preprocessor for the EQ3/6 Software Package: User's Guide and Related Documentation (Version 7.0)*. UCRL-MA-110662 PT II. Lawrence Livermore National Laboratory, Livermore, California.

Deng, H., S. Johnsen, Y. Xiong, G.T. Roselle, and M. Nemer, 2006a. *Analysis of Martin Marietta MagChem® 10 WTS-60 MgO*. Sandia National Laboratories, Carlsbad, New Mexico. ERMS 544712.

Deng, H., M.B. Nemer, and Y. Xiong, 2006b. *Experimental Study of MgO Reaction Pathways and Kinetics*. Sandia National Laboratories, TP 06-03, Rev. 0, Carlsbad, New Mexico, June 6, 2006. ERMS 543633.

Detwiler, R.P., 2004. *MgO Emplacement*. Letter from R.P. Detwiler, Acting Manager, U.S. DOE Carlsbad Field Office, to E. Cotsworth, Director, Office of Radiation and Indoor Air, U.S. EPA, dated October 20, 2004.

DOE (U.S. Department of Energy) 1996. *Title 40 CFR Part 191 Compliance Certification Application for the Waste Isolation Pilot Plant*, DOE/CAO-1996-2184, October 1996, Carlsbad Field Office, Carlsbad, New Mexico.

DOE (U.S. Department of Energy) 2004. Title 40 CFR 191 Parts B and C Compliance Recertification Application, U.S. Department of Energy Field Office, March 2004. Docket A-98-49 Category II-B2.

EPA (Environmental Protection Agency) 1997. *Compliance Application Review Documents for the Criteria for the Certification and Recertification of the Waste Isolation Pilot Plant's Compliance with the 40 CFR Part 191 Disposal Regulations: Final Certification Decision. CARD 44: Engineered Barrier*. U.S. Environmental Protection Agency Office of Radiation and Indoor Air. Washington, DC. Docket A-93-02 Item V-B-2.

EPA (Environmental Protection Agency) 1998a. Criteria for the Certification and Recertification of the Waste Isolation Pilot Plant's Compliance with the Disposal Regulations: Certification Decision; Final Rule. *Federal Register* 63(95):27354-27406, May 18.

EPA (U.S. Environmental Protection Agency) 1998b. *Final WIPP Certification Decision Response to Comments, Criteria for the Certification of the Waste Isolation Pilot Plant's Compliance with 40 CFR Part 191 Disposal Regulations: Certification Decision.* Office of Radiation and Indoor Air, Washington, DC. Docket No. A-93-02 Item V-C-1.

EPA (Environmental Protection Agency) 1998c. *Technical Support Document for Section 194.24: EPA's Evaluation of DOE's Actinide Source Term.* Environmental Protection Agency, Office of Radiation and Indoor Air, Washington, DC. Docket A-93-02 Item V-B-17.

EPA (Environmental Protection Agency) 2001. *Approval of Elimination of Minisacks.* Environmental Protection Agency Office of Radiation and Indoor Air, Washington, DC., Docket A-98-49 Item II-B-3, Item 15.

EPA (Environmental Protection Agency) 2006a. Criteria for the Certification and Recertification of the Waste Isolation Pilot Plant's Compliance with the Disposal Regulations: Recertification Decision. *Federal Register* 71(68):18010-18021, April 10.

EPA (Environmental Protection Agency) 2006b. *Technical Support Document for Section 194.24: Evaluation of the Compliance Recertification Actinide Source Term and Culebra Dolomite Distribution Coefficient Values.* Office of Radiation and Indoor Air, Docket No: A-98-49, March 2006.

Evans, G., V. Schmidt, P. Bush, and H. Nelson, 1969. Stratigraphy and geologic history of the sabkha, Abu Dhabi, Persian Gulf. *Sedimentology* 12:145-159.

Graf, D.L., A.J. Eardley, and N.F. Shimp, 1961. A preliminary report on magnesium carbonate formation in Glacial Lake Bonneville. *Journal of Geology* 69:219-223.

Gitlin, B.C. 2006. U.S. Environmental Protection Agency, Office of Air and Radiation, Washington, DC. Letter to D.C. Moody, U.S. Department of Energy, Carlsbad Field Office, Carlsbad, New Mexico. April 28, 2006.

IMA (International Mineralogical Association) 2007. *IMA/CNMC List of Mineral Names.* Compiled by E.H. Nickel and M.E. Nichols, June 5, 2007. Accessed July 13, 2007 at http://www.geo.vu.nl/users/ima-cnmmn/MINERALlist.pdf.

Irion, G., and G. Müller, 1968. Huntite, dolomite, magnesite, and polyhalite of recent age from Tuz Gölü, Turkey. *Nature* 220:130-131.

Kanney, J.F., A.C. Snider, T.W. Thompson, and L.H. Brush, 2004. *Effect of Naturally Occurring Sulfate on the MgO Safety Factor in the Presence of Supercompacted Waste and Heterogeneous Waste Emplacement.* Sandia National Laboratories, Carlsbad Programs Group, Carlsbad, New Mexico. March 5, 2004.

Kanney, J.F. and E.D. Vugrin, 2006. *Updated Analysis of Characteristic Time and Length Scales for Mixing Processes in the WIPP Repository to Reflect the CRA-2004 PABC Technical Baseline and the Impact of Supercompacted Mixed Waste and Heterogeneous Waste*

Emplacement. Memorandum to D.S. Kessel, Sandia National Laboratories, Carlsbad, New Mexico, August 31, 2006.

Kirchner, T., and E. Vugrin, 2006. *Uncertainty in Cellulose, Plastic, and Rubber Measurements for the Waste Isolation Pilot Plant Inventory.* Sandia National Laboratories, Carlsbad, New Mexico. ERMS 543848.

Königsberger, E., L.C. Königsberger, and H. Gamjäger, 1999. Low-temperature thermodynamic model for the system Na_2CO_3-$MgCO_3$-$CaCO_3$-H_2O. *Geochimica et Cosmochimica Acta* 63:3105-3119.

Krumhansl, J.L., Kelly, J.W., Papenguth, H.W., and R.V. Bynum, 1997. *MgO Acceptance Criteria*. Memorandum to E.J. Nowak, December 10, 1997. Sandia National Laboratories, Albuquerque, New Mexico. ERMS 248997. Docket A-98-49 Item II-B2-39.

Lambert, S.J., 1992. Geochemistry of the Waste Isolation Pilot Plant (WIPP) site, southeastern New Mexico, USA. *Applied Geochemistry* 7:513-531.

Langmuir, D., 1965. Stability of Carbonates in the System MgO-CO_2-H_2O. *Journal of Geology* 73:730-754.

Langmuir, D., 2007. *Letter Report Review of the SC&A Draft Report "Review of MgO-Related Uncertainties in the Waste Isolation Pilot Plant". Contract No. EP-D-05-002, Work Assignment No. 3-07.* Prepared for the U.S. Environmental Protection Agency, Washington DC, December 2007.

Leigh, C., 2005. *Calculation of Moles of Sulfate and Nitrate for Performance Assessment Baseline Calculation.* Sandia National Laboratories, Carlsbad, New Mexico. ERMS 539331.

Leigh, C., J. Kanney, L. Brush, J. Garner, R. Kirkes, T. Lowry, M. Nemer, J. Stein, E. Vugrin, S. Wagner, and T. Kirchner, 2005a. *2004 Compliance Recertification Application Performance Assessment Baseline Calculation.* Sandia National Laboratories, Carlsbad, New Mexico. ERMS 541521.

Leigh, C., J. Trone, and B. Fox, 2005b. *TRU Waste Inventory for the 2004 Compliance Recertification Application Performance Assessment Baseline Calculation.* Sandia National Laboratories, Carlsbad, New Mexico. ERMS 541118

Lippmann, F., 1973. *Sedimentary Carbonate Minerals.* Springer-Verlag, New York.

Lynd, L.R., P.J. Weimer, W.H. van Zyl, and I.S. Pretorius, 2002. Microbial cellulose utilization: fundamentals and biotechnology. *Microbiology and Molecular Biology Reviews* 66:506–577.

Marcinowski, F., 2004. Letter from F. Marcinowski, U.S. Environmental Protection Agency Radiation Protection Division to R.P. Detwiler, U.S. Department of Energy Carlsbad Field Office, dated March 26, 2004.

Martin Marietta 2006. *MagChem® Analysis of Shipment*. Martin Marietta Magnesia Specialties LLC, May 16, 2006. ERMS 543900.

Meldrum, F.C., and S.T. Hyde, 2001. Morphological influence of magnesium and organic additives on the precipitation of calcite. *Journal of Crystal Growth* 231:544-558.

Moody, D.C., 2006. U.S. Department of Energy, Carlsbad Field Office, Letter to E.A. Cotsworth, U.S. Environmental Protection Agency, requesting a reduction in the MgO Excess Factor from 1.67 to 1.2. April 10, 2006. ERMS 543262.

Moody, D.C., 2007. U.S. Department of Energy, Carlsbad Field Office, Letter to J. Reyes, U.S. Environmental Protection Agency, requesting that the Brush et al. (2006) report not be used as part of the technical basis for EPA's decision process on the MgO Planned Change Request. November 21, 2006.

Nemer, M.B., 2007. *Effects of Not Including Emplacement Materials in CPR Inventory on Recent PA Results.* Sandia National Laboratories, Carlsbad, New Mexico. ERMS 545689.

Patterson, R., 2007. *Chemical Analysis of the MagChem 10 WTS 60 as Supplied to the Waste Isolation Pilot Plant.* Letter plus enclosures from U.S. Department of Energy Carlsbad Field Office to J. Reyes, U.S. Environmental Protection Agency Office of Radiation and Indoor Air, July 10, 2007.

Pettersen, R.C., 1984. The chemical composition of wood. In: Rowell, R. (Ed.) *Chemistry of Solid Wood*, Advances in Chemistry Series 207, American Chemical Society, Washington, DC. pp. 57–126.

Renaut, R.W. and D. Stead, 1990. Recent Magnesite-hydromagnesite sedimentation in playa basins of the Cariboo Plateau, British Columbia. *Geological Fieldwork 1990*, *Paper 1991-1,* pp. 279–288.

Sayles, F.L, and W.S. Fyfe, 1973. The crystallization of magnesite from aqueous solution. *Geochimica et Cosmochimica Acta* 37:87-99.

SCA (S. Cohen and Associates) 2006a. *Preliminary Review of the Degradation of Cellulosic, Plastic, and Rubber Materials in the Waste Isolation Pilot Plant, and Possible Effects on Magnesium Oxide Safety Factor Calculations.* Prepared for the U.S. Environmental Protection Agency, August 21.

SCA (S. Cohen and Associates) 2006b. *Technical Support for the Recertification and Continuing Compliance of the Waste Isolation Pilot Plant, TD2006-4 Waste Characterization Uncertainty Measurement.* Prepared for the U.S. Environmental Protection Agency, September 26.

SCA (S. Cohen and Associates) 2008. *Response to Comments by Langmuir (2007).* Technical Memorandum to file, January 14, 2008.

Snider, A.C., 2001. MgO Hydration Experiments Conducted at SNL/ABQ. *Sandia National Laboratories Technical Baseline Reports, WBS 1.3.5.4, Repository Investigations, Milestone RI020, July 31, 2001.* Sandia National Laboratories, Carlsbad, New Mexico. ERMS 518970, pp. 4-1 to 4-3.

Snider, A.C., 2002. MgO Studies: Experimental Work Conducted at SNL/Carlsbad. Efficacy of Premier Chemicals MgO as an Engineered Barrier, *Sandia National Laboratories Technical Baseline Reports, WBS 1.3.5.3, Compliance Monitoring; WBS 1.3.5.4, Repository Investigations, Milestone RI110, January 31, 2002.* Sandia National Laboratories, Carlsbad, New Mexico. ERMS 520467, pp. 3.1-1 to 3.1-18.

Snider, A.C., 2003. Hydration of Magnesium Oxide in the Waste Isolation Pilot Plant. *Sandia National Laboratories Technical Baseline Reports, WBS 1.3.5.3, Compliance Monitoring; WBS 1.3.5.4, Repository Investigations, Milestone RI 03-210, January 31, 2003.* Sandia National Laboratories, Carlsbad, New Mexico. Pages 4.2-1 to 4.2-6, ERMS 526049.

Snider, A.C., and Y. L. Xiong, 2002. Carbonation of Magnesium Oxide, *Sandia National Laboratories Technical Baseline Reports, WBS 1.3.5.3, Compliance Monitoring; WBS 1.3.5.4, Repository Investigations, Milestone RI130, July 31, 2002.* Sandia National Laboratories, Carlsbad, New Mexico. ERMS 523189, pp. 4.1-1 to 4.1-28.

SNL (Sandia National Laboratories) 1997. *Chemical Conditions Model: Results of the MgO Backfill Efficacy Investigation.* Prepared for the U.S. Department of Energy, Carlsbad Area Office, April 23, 2007. Docket No. A-93-02 Item II-A-39.

Stamatakis, M.G., 1995. Occurrence and genesis of huntite-hydromagnesite assemblages, Kozani, Greece– important new white fillers and extenders. *Applied Earth Science* 104:B179-B210.

Stein, C.L., 1985. *Mineralogy in the Waste Isolation Pilot Plant (WIPP) Facility Stratigraphic Horizon.* Sandia National Laboratories, SAND85-0321, Albuquerque, New Mexico.

TEA (Trinity Engineering Associates) 2004. *Review of Effects of Supercompacted Waste and Heterogeneous Waste Emplacement on WIPP Repository Performance. Final Report.* Prepared for U.S. Environmental Protection Agency, Office of Radiation and Indoor Air, Washington, DC, March 17, 2004.

Thompson, J.B., and F.G. Ferris, 1990. Cyanobacterial precipitation of gypsum, calcite and magnesite from natural lake water. *Geology* 18:995-998.

Triay, I., 2002. Letter from Dr. I. Triay, Manager, U.S. Department of Energy Carlsbad Field Office, to F. Marcinowski, Director, U.S. Environmental Protection Agency Radiation Protection Division, dated December 10, 2002. (Docket A-98-49, Item II-B-15).

Usdowski, E., 1994. Synthesis of dolomite and geochemical implications. *Spec. Publs. Inst. Ass. Sediment.* 21:345-360.

Vance, R.E., R.W. Mathewes, and J.J. Clague, 1992. 7000-year record of lake-level change on the northern Great Plains: a high-resolution proxy of past climate. *Geology* 20:879-882.

von der Borch, C., 1965. The distribution and preliminary geochemistry of modern carbonate sediments of the Coorong area, South Australia. *Geochimica et Cosmochimica Acta* 29:781-799.

Vugrin, E.D., M.B. Nemer, and S. Wagner, 2006. *Uncertainties Affecting MgO Effectiveness and Calculation of the MgO Effective Excess Factor.* Revision 0, Sandia National Laboratories, Carlsbad, New Mexico.

Vugrin, E.D., M.B. Nemer, and S. Wagner, 2007. *Uncertainties Affecting MgO Effectiveness and Calculation of the MgO Effective Excess Factor.* Revision 1, Sandia National Laboratories, Carlsbad, New Mexico. ERMS 546377.

Wall, N.A., 2005. *Preliminary Results for the Evaluation of Potential New MgO.* Sandia National Laboratories, Carlsbad, New Mexico. ERMS 538514.

Wall, N.A., and D. Enos, 2006. *Iron and Lead Corrosion in WIPP-Relevant Conditions.* TP 06-02, Rev. 1. Sandia National Laboratories, Carlsbad, New Mexico, April 24, 2006. ERMS 543238.

Wang, Y., 2000. *Effectiveness of Mixing Processes in the Waste Isolation Pilot Plant Repository.* Technical Memorandum, Sandia National Laboratories, Carlsbad, New Mexico. ERMS 512401.

Wang, Y. and LH. Brush, 1996. *Estimates of Gas-Generation Parameters for the Long-Term WIPP Performance Assessment.* Unpublished memorandum to M.S. Tierney, Sandia National Laboratories, Albuquerque, New Mexico, January 26, 1996. WPO 31943. ERMS 231943

Wilson, C., D. Porter, J. Gibbons, E. Oswald, G. Sjoblom, and F. Caporuscio, 1996a. *Conceptual Models Peer Review Report*, Prepared for the U.S. Department of Energy, Carlsbad, New Mexico, July 1996. Docket No. A-93-02 Item II-G-1.

Wilson, C., D. Porter, J. Gibbons, E. Oswald, G. Sjoblom, and F. Caporuscio, 1996b. *Conceptual Models Supplementary Peer Review Report*, Prepared for the U.S. Department of Energy, Carlsbad, New Mexico, December 1996. Docket No. A-93-02 Item II-G-12.

Wilson, C., D. Porter, J. Gibbons, E. Oswald, G. Sjoblom, and F. Caporuscio, 1997a. *Conceptual Models Second Supplementary Peer Review Report*, Prepared for the U.S. Department of Energy, Carlsbad, New Mexico, January 1997. Docket No. A-93-02 Item II-G-21.

Wilson, C., D. Porter, J. Gibbons, E. Oswald, G. Sjoblom, and F. Caporuscio, 1997b. *Conceptual Models Third Supplementary Peer Review Report*, Prepared for the U.S. Department of Energy, Carlsbad, New Mexico, April 1997. Docket No. A-93-02 Item II-G-22.

Wolery, T.J., 1992a. *EQ3/6, A Software Package for Geochemical Modeling of Aqueous Systems: Package Overview and Installation Guide (Version 7.0).* UCRL-MA-110662 PT I. Lawrence Livermore National Laboratory, Livermore, California.

Wolery, T.J., 1992b. *EQ3NR, A Computer Program for Geochemical Aqueous Speciation-Solubility Calculations: Theoretical Manual, User's Guide, and Related Documentation (Version 7.0).* UCRL-MA-110662 PT III. Lawrence Livermore National Laboratory, Livermore, California.

Wolery, T.J., and S.A. Daveler, 1992. *EQ6, A Computer Program for Reaction-Path Modeling of Aqueous Geochemical Systems: Theoretical Manual, User's Guide, and Related Documentation (Version 7.0).* UCRL-MA-110662 PT IV. Lawrence Livermore National Laboratory, Livermore, California.

WTS (Washington TRU Solutions) 2005. *Specifications for Repackaged Backfill*. Waste Isolation Pilot Plant Procedure D-0101, Revision 7, May 2005.

Xiong, Y.-L., and A.C. Snider, 2003. Carbonation Rates of the Magnesium Oxide Hydration Product Brucite in Various Solutions. *Sandia National Laboratories Technical Baseline Reports, WBS 1.3.5.4, Repository Investigations, Milestone RI 03-210, January 31, 2003.* Sandia National Laboratories, Carlsbad, New Mexico. ERMS 526049, pp. 4.3-1 to 4.3-11.

Zhang, P.-C., H.L. Anderson, J.W. Kelly, J.L. Krumhansl, and H.W. Papenguth, 2000. Kinetics and mechanisms of formation of magnesite from hydromagnesite in brine. Submitted to *Applied Geochemistry*. Sandia National Laboratories, Albuquerque, New Mexico. ERMS 514868.

Zhang, P., J. Hardesty, and H. Papenguth, 2001. MgO Hydration Experiments Conducted at SNL-ABQ. *Sandia National Laboratories Technical Baseline Reports, WBS 1.3.5.4, Compliance Monitoring; WBS 1.3.5.4, Repository Investigations, Milestone RI010, January 31, 2001*. Sandia National Laboratories, Carlsbad, New Mexico. ERMS 516749, pp. 55–65.

APPENDIX A: WTS-60 MAGNESIUM OXIDE INFORMATION FROM MARTIN MARIETTA MAGNESIA SPECIALTIES

Martin Marietta Specifications Sheet for WTS-60 MgO

Hard Burned Technical Grade Magnesium Oxide

DESCRIPTION	MagChem® 10 grades are high purity technical grades of magnesium oxide processed from magnesium-rich brine. They have relatively high density and low reactivity. The granular grades are essentially dust free.
USES	Milled MagChem 10 grades have a combination of low reactivity, high purity and fine particle size, which makes them suitable for the production of magnesium salts, particularly in reaction with strong acids. Milled MagChem 10 grades also find applications in fiberglass, aluminum metal processing and fuel additives. Screened MagChem 10 products are widely used as a raw material in manufacturing refractories and ceramic products.

COMPOSITION

	Typical	Specifications	
Magnesium Oxide (MgO), %	98.2	97.0	min.
Calcium Oxide (CaO), %	0.9	1.0	max.
Silicon Oxide (SiO_2), %	0.4	0.5	max.
Iron Oxide (Fe_2O_3), %	0.2	0.3	max.
Aluminum Oxide (Al_2O_3), %	0.1	0.2	max.
Chloride (Cl), %	0.01	0.02	max.
Sulfate (SO_3), %	0.01	0.02	max.
Loss on Ignition, %	0.25	0.5	max.

MagChem 10 grades are available in a wide variety of screened and milled sizes, from a powder minus 325 mesh to a granular 6 X 16 mesh. Loose bulk densities range from 65 to 120 lb/ft^3.

Screened Grades

Grade	Top Size % Passing, min.		Bottom Size % Passing, max.	
6 X 16	98	-6 mesh	10	-16 mesh
12 X 40	95	-12 mesh	10	-40 mesh
PR-30	98	-16 mesh	15	-100 mesh

Milled Grades

Grade	Top Size % Passing, min.		Median Particle Size, Microns
-20 *	96	-20 mesh	50
-200	95	-200 mesh	10
-325	96	-325 mesh	10
-325S	99	-325 mesh	9

PACKAGING	Available in bulk carload, truckload, and 2000-lb bulk sacks. * Bulk carloads and truckloads only.
STORAGE	Store in dry place. Exposure to moisture may cause caking.

WTS-60 Brine Feed Chemistry Data (from Patterson 2007)

Brine Feed Chemistry Summary 2004-2007 ANALYSIS of "C"
HEAD TANK BRINE 2004 - 2007

2004:	CaCl2	MgCl2	NaCl	pH	Specific Gravity
Average:	208	108	44	5.13	1.272
Std. Dev.:	5	5	1	0.12	0.004
Variance:	21	27	2	0.02	0.00002
Max:	216	135	50	5.52	1.280
Min:	197	99.2	41.3	4.97	1.261

2005:					
Average:	211	110	45	5.07	1.271
Std. Dev.:	4	3	1	0.16	0.002
Variance:	16	7	1	0.02	0.000004
Max:	219	119	47	5.70	1.280
Min:	196	105	41	4.84	1.267

2006:					
Average:	210	107	45	5.07	1.265
Std. Dev.:	5	4	1	0.08	0.004
Variance:	20	15	2	0.01	0.00001
Max:	222	115	48	5.26	1.275
Min:	198	99	42	4.88	1.258

2007:	(Through 6/14/07)				
Average:	208	108	44	5.00	1.270
Std. Dev.:	5	3	2	0.05	0.002
Variance:	26	7	3	0.003	0.000004
Max:	220	113	47	5.11	1.272
Min:	198	103	42	4.86	1.263

Averages

	Avg. CaCl2	Avg. MgCl2	Avg. NaCl	Avg. pH	Avg. Specific Gravity
2004	208	108	44	5.13	1.272
2005	211	110	45	5.07	1.271
2006	210	107	45	5.07	1.265
2007	208	108	44	5.00	1.270

WTS-60 Dolime Feed Chemistry Summary 2004 to 2007
(from Patterson 2007)

LOAD DATE	CAO	MGO	SIO2	FE2O3	AL2O3
23-Jan-04	56.5	40.4	0.27	0.14	0.10
23-Jan-04	56.8	41.2	0.33	0.15	0.08
30-Jan-04	56.5	40.2	0.49	0.24	0.12
31-Jan-04	56.4	40.5	0.27	0.12	0.07
10-Feb-04	58.2	40.3	0.35	0.18	0.12
11-Feb-04	58.2	40.3	0.32	0.17	0.11
18-Feb-04	58.4	40.5	0.37	0.16	0.13
18-Feb-04	58.4	40.5	0.25	0.15	0.09
22-Feb-04	58.3	40.4	0.27	0.13	0.10
24-Feb-04	58.3	40.4	0.25	0.13	0.08
04-Mar-04	58.4	40.5	0.26	0.16	0.09
04-Mar-04	58.4	40.5	0.25	0.14	0.09
08-Mar-04	58.3	40.4	0.35	0.14	0.10
10-Mar-04	58.3	40.4	0.32	0.14	0.11
14-Mar-04	58.2	40.3	0.41	0.23	0.14
16-Mar-04	58.2	40.3	0.45	0.20	0.16
06-Apr-04	58.3	40.4	0.38	0.18	0.11
06-Apr-04	58.3	40.4	0.34	0.18	0.11
14-Apr-04	58.5	40.5	0.38	0.17	0.11
13-Apr-04	58.5	40.5	0.32	0.15	0.09
18-Apr-04	58.4	40.4	0.33	0.16	0.11
18-Apr-04	58.4	40.4	0.26	0.09	0.07
28-Apr-04	58.3	40.5	0.37	0.19	0.12
29-Apr-04	58.3	40.5	0.28	0.12	0.10
03-May-04	58.2	40.3	0.28	0.14	0.08
03-May-04	58.2	40.3	0.29	0.14	0.09
09-May-04	58.2	40.3	0.32	0.13	0.10
09-May-04	58.2	40.3	0.37	0.18	0.11
16-May-04	58.2	40.3	0.20	0.13	0.07
16-May-04	58.2	40.3	0.33	0.16	0.11
23-May-04	58.2	40.3	0.34	0.19	0.12
24-May-04	58.2	40.3	0.45	0.26	0.15
30-May-04	58.0	40.2	0.41	0.14	0.15
31-May-04	58.0	40.2	0.47	0.23	0.14
23-Jun-04	58.3	40.4	0.44	0.18	0.15
23-Jun-04	58.3	40.4	0.43	0.17	0.14
08-Jul-04	57.8	40.1	0.44	0.16	0.14
08-Jul-04	57.8	40.1	0.29	0.09	0.10
14-Jul-04	58.0	40.2	0.32	0.14	0.12
14-Jul-04	58.4	40.4	0.29	0.11	0.10
20-Jul-04	58.1	40.2	0.56	0.25	0.17
22-Jul-04	58.1	40.2	0.51	0.20	0.14
26-Jul-04	58.3	40.3	0.39	0.16	0.13
27-Jul-04	58.4	40.4	0.41	0.17	0.14
04-Aug-04	58.3	40.4	0.60	0.24	0.21
04-Aug-04	58.4	40.5	0.43	0.20	0.13
12-Aug-04	58.2	40.3	0.34	0.13	0.12
12-Aug-04	58.3	40.4	0.34	0.13	0.10
15-Aug-04	58.1	40.3	0.21	0.13	0.07
16-Aug-04	58.1	40.3	0.40	0.23	0.15
23-Aug-04	58.4	40.5	0.36	0.19	0.12

WTS-60 Dolime Feed Chemistry Summary 2004 to 2007 (contd)
(from Patterson 2007)

LOAD DATE	CAO	MGO	SIO2	FE2O3	AL2O3
25-Aug-04	58.4	40.5	0.44	0.21	0.12
02-Sep-04	58.4	40.4	0.26	0.10	0.10
02-Sep-04	58.3	40.3	0.27	0.17	0.10
09-Sep-04	58.3	40.4	0.45	0.18	0.13
10-Sep-04	58.3	40.4	0.27	0.09	0.10
13-Sep-04	58.3	40.4	0.38	0.18	0.14
18-Sep-04	58.3	40.4	0.33	0.15	0.10
23-Sep-04	58.6	40.5	0.37	0.19	0.10
30-Sep-04	58.6	40.5	0.32	0.16	0.10
04-Oct-04	58.2	40.3	0.31	0.17	0.09
04-Oct-04	58.2	40.3	0.34	0.16	0.08
15-Oct-04	58.5	40.5	0.40	0.20	0.11
15-Oct-04	58.5	40.5	0.43	0.20	0.15
20-Oct-04	58.6	40.6	0.24	0.14	0.08
20-Oct-04	58.4	40.4	0.35	0.20	0.11
25-Oct-04	58.1	40.3	0.29	0.21	0.10
26-Oct-04	58.6	40.6	0.34	0.12	0.14
31-Oct-04	58.1	40.2	0.28	0.18	0.08
31-Oct-04	58.1	40.2	0.38	0.23	0.11
10-Nov-04	58.7	40.6	0.17	0.13	0.06
10-Nov-04	58.7	40.6	0.23	0.18	0.08
15-Nov-04	58.2	40.3	0.27	0.13	0.08
15-Nov-04	58.6	40.6	0.22	0.13	0.07
22-Nov-04	58.4	40.4	0.26	0.16	0.09
21-Nov-04	58.2	40.3	0.35	0.15	0.09
01-Dec-04	58.2	40.3	0.39	0.12	0.09
29-Nov-04	58.5	40.5	0.28	0.14	0.09
05-Dec-04	58.6	40.6	0.23	0.13	0.08
07-Dec-04	58.1	40.3	0.38	0.19	0.11
17-Dec-04	58.1	40.3	0.20	0.14	0.08
17-Dec-04	58.3	40.5	0.25	0.20	0.09
21-Dec-04	58.4	40.5	0.31	0.19	0.11
21-Dec-04	58.3	40.4	0.31	0.20	0.13
25-Dec-04	57.7	40.0	0.23	0.14	0.08
29-Dec-04	58.5	40.5	0.36	0.16	0.13
06-Jan-05	58.5	40.5	0.31	0.18	0.11
06-Jan-05	58.3	40.4	0.26	0.15	0.09
07-Jan-05	58.1	40.2	0.29	0.12	0.08
09-Jan-05	58.2	40.3	0.27	0.14	0.07
21-Jan-05	58.4	40.5	0.24	0.14	0.08
21-Jan-05	58.6	40.6	0.27	0.18	0.10
26-Jan-05	58.4	40.4	0.26	0.17	0.09
26-Jan-05	58.5	40.5	0.31	0.22	0.12
30-Jan-05	58.5	40.5	0.33	0.20	0.13
02-Feb-05	58.1	40.2	0.30	0.15	0.09
07-Feb-05	58.6	40.6	0.29	0.15	0.10
06-Feb-05	58.4	40.5	0.32	0.15	0.11
15-Feb-05	58.6	40.6	0.31	0.17	0.11
17-Feb-05	58.4	40.5	0.24	0.15	0.09
20-Feb-05	58.0	40.2	0.15	0.08	0.05
21-Feb-05	58.1	40.2	0.18	0.10	0.07
27-Feb-05	58.5	40.5	0.29	0.17	0.10
03-Mar-05	58.3	40.4	0.30	0.16	0.10
10-Mar-05	57.9	40.1	0.25	0.15	0.10
11-Mar-05	57.9	40.1	0.24	0.13	0.09

WTS-60 Dolime Feed Chemistry Summary 2004 to 2007 (contd)
(from Patterson 2007)

LOAD DATE	CAO	MGO	SIO2	FE2O3	AL2O3
18-Mar-05	58.2	40.3	0.39	0.19	0.13
18-Mar-05	58.3	40.4	0.35	0.16	0.11
20-Mar-05	58.5	40.5	0.30	0.17	0.10
20-Mar-05	58.4	40.5	0.30	0.16	0.10
30-Mar-05	58.1	40.2	0.33	0.15	0.13
30-Mar-05	57.9	40.1	0.29	0.14	0.12
05-Apr-05	58.7	40.7	0.23	0.12	0.09
07-Apr-05	58.3	40.4	0.26	0.10	0.07
13-Apr-05	58.2	40.3	0.22	0.11	0.06
13-Apr-05	58.2	40.3	0.24	0.11	0.06
22-Apr-05	58.4	40.5	0.32	0.09	0.09
22-Apr-05	58.4	40.4	0.36	0.08	0.08
24-Apr-05	57.7	39.9	0.28	0.12	0.10
26-Apr-05	58.4	40.4	0.30	0.14	0.10
06-May-05	58.4	40.4	0.22	0.11	0.07
06-May-05	58.3	40.4	0.25	0.14	0.08
10-May-05	58.0	40.1	0.30	0.14	0.09
12-May-05	58.5	40.5	0.27	0.13	0.08
16-May-05	58.3	40.4	0.32	0.18	0.11
16-May-05	58.1	40.3	0.29	0.14	0.10
21-May-05	58.2	40.3	0.16	0.11	0.06
25-May-05	57.8	40.0	0.20	0.12	0.08
02-Jun-05	58.6	40.6	0.34	0.15	0.09
02-Jun-05	58.4	40.4	0.46	0.22	0.13
09-Jun-05	57.6	39.9	0.35	0.17	0.12
10-Jun-05	58.2	40.3	0.35	0.13	0.08
13-Jun-05	57.7	40.0	0.27	0.16	0.10
13-Jun-05	57.6	39.9	0.37	0.13	0.15
21-Jun-05	58.2	40.3	0.32	0.16	0.09
22-Jun-05	58.4	40.5	0.35	0.16	0.11
25-Jun-05	58.2	40.3	0.31	0.16	0.10
29-Jun-05	58.5	40.5	0.24	0.13	0.07
11-Jul-05	58.6	40.6	0.19	0.10	0.07
11-Jul-05	58.1	40.3	0.27	0.13	0.08
13-Jul-05	58.6	40.6	0.26	0.15	0.09
13-Jul-05	57.9	40.1	0.25	0.14	0.08
17-Jul-05	58.3	40.5	0.30	0.17	0.12
18-Jul-05	57.6	40.0	0.21	0.10	0.08
23-Jul-05	58.5	40.5	0.27	0.15	0.10
24-Jul-05	58.6	40.6	0.22	0.14	0.08
05-Aug-05	58.4	40.4	0.36	0.18	0.03
05-Aug-05	58.4	40.5	0.32	0.18	0.20
10-Aug-05	58.0	40.2	0.33	0.15	0.11
15-Aug-05	58.6	40.6	0.31	0.19	0.12
15-Aug-05	58.6	40.6	0.32	0.19	0.12
25-Aug-05	57.8	40.1	0.38	0.17	0.12
25-Aug-05	58.3	40.4	0.28	0.15	0.11
30-Aug-05	58.2	40.3	0.38	0.19	0.12
31-Aug-05	57.6	39.9	0.25	0.10	0.06
07-Sep-05	58.4	40.4	0.41	0.19	0.14
07-Sep-05	58.5	40.5	0.31	0.17	0.12
13-Sep-05	57.7	40.0	0.25	0.10	0.08
15-Sep-05	58.2	40.3	0.36	0.19	0.13
21-Sep-05	58.4	40.4	0.41	0.16	0.09
21-Sep-05	58.1	40.3	0.35	0.16	0.11

WTS-60 Dolime Feed Chemistry Summary 2004 to 2007 (contd)
(from Patterson 2007)

LOAD DATE	CAO	MGO	SIO2	FE2O3	AL2O3
28-Sep-05	58.5	40.5	0.32	0.14	0.10
28-Sep-05	58.5	40.5	0.27	0.15	0.09
05-Oct-05	58.5	40.5	0.34	0.14	0.10
05-Oct-05	58.2	40.3	0.31	0.14	0.10
10-Oct-05	58.5	40.5	0.37	0.11	0.16
11-Oct-05	58.3	40.4	0.37	0.13	0.17
18-Oct-05	58.1	40.2	0.34	0.17	0.12
19-Oct-05	58.1	40.2	0.51	0.19	0.14
22-Oct-05	57.8	40.0	0.33	0.18	0.11
23-Oct-05	58.4	40.4	0.39	0.14	0.09
02-Nov-05	58.6	40.6	0.27	0.15	0.09
02-Nov-05	58.4	40.4	0.28	0.14	0.08
10-Nov-05	58.3	40.4	0.33	0.16	0.14
08-Nov-05	58.5	40.5	0.33	0.19	0.12
17-Nov-05	58.6	40.6	0.21	0.13	0.08
15-Nov-05	58.0	40.2	0.29	0.14	0.11
20-Nov-05	58.2	40.3	0.16	0.06	0.04
21-Nov-05	57.7	40.0	0.18	0.10	0.06
29-Nov-05	58.4	40.4	0.39	0.19	0.14
29-Nov-05	58.4	40.4	0.28	0.20	0.10
04-Dec-05	57.2	39.6	0.15	0.07	0.04
05-Dec-05	57.7	39.9	0.27	0.11	0.08
16-Dec-05	58.3	40.4	0.35	0.21	0.14
16-Dec-05	58.4	40.4	0.27	0.15	0.10
24-Dec-05	58.6	40.6	0.34	0.19	0.11
25-Dec-05	58.2	40.3	0.43	0.16	0.10
05-Jan-06	58.4	40.5	0.26	0.20	0.09
05-Jan-06	58.4	40.5	0.36	0.19	0.11
10-Jan-06	58.6	40.6	0.24	0.16	0.09
11-Jan-06	57.9	40.1	0.32	0.17	0.11
17-Jan-06	58.4	40.4	0.44	0.23	0.15
18-Jan-06	57.6	39.9	0.27	0.27	0.10
24-Jan-06	58.4	40.4	0.35	0.09	0.24
01-Feb-06	57.9	40.1	0.35	0.11	0.13
01-Feb-06	58.1	40.3	0.31	0.23	0.14
08-Feb-06	58.7	40.7	0.21	0.12	0.08
08-Feb-06	58.4	40.5	0.37	0.25	0.12
15-Feb-06	57.6	39.9	0.42	0.22	0.14
16-Feb-06	58.1	40.2	0.36	0.20	0.14
20-Feb-06	58.0	40.2	0.47	0.33	0.18
20-Feb-06	58.4	40.4	0.46	0.33	0.18
26-Feb-06	58.0	40.1	0.23	0.17	0.08
26-Feb-06	58.3	40.4	0.32	0.20	0.11
08-Mar-06	58.3	40.4	0.14	0.11	0.05
09-Mar-06	58.6	40.6	0.21	0.13	0.07
18-Mar-06	58.3	40.4	0.18	0.09	0.06
19-Mar-06	58.4	40.5	0.18	0.10	0.06
23-Mar-06	58.0	40.2	0.23	0.11	0.07
26-Mar-06	58.7	40.6	0.24	0.14	0.07
29-Mar-06	58.5	40.5	0.37	0.18	0.13
29-Mar-06	58.6	40.6	0.31	0.17	0.11
07-Apr-06	58.4	40.4	0.32	0.17	0.12
06-Apr-06	58.5	40.5	0.22	0.13	0.08
09-Apr-06	58.7	40.7	0.19	0.14	0.07
09-Apr-06	58.1	40.2	0.18	0.24	0.07

WTS-60 Dolime Feed Chemistry Summary 2004 to 2007 (contd)
(from Patterson 2007)

LOAD DATE	CAO	MGO	SIO2	FE2O3	AL2O3
16-Apr-06	58.3	40.4	0.42	0.17	0.10
28-Apr-06	58.7	40.6	0.22	0.12	0.08
28-Apr-06	58.5	40.5	0.21	0.13	0.07
04-May-06	58.6	40.6	0.27	0.13	0.08
05-May-06	58.0	40.2	0.23	0.12	0.07
08-May-06	57.5	39.8	0.24	0.11	0.07
08-May-06	58.4	40.4	0.39	0.21	0.13
15-May-06	57.6	39.9	0.26	0.15	0.08
15-May-06	58.6	40.6	0.22	0.14	0.08
24-May-06	58.6	40.6	0.28	0.14	0.08
24-May-06	57.8	40.0	0.30	0.18	0.09
30-May-06	57.6	39.9	0.31	0.18	0.11
30-May-06	58.6	40.6	0.31	0.15	0.09
04-Jun-06	58.4	40.5	0.22	0.11	0.08
04-Jun-06	58.5	40.5	0.23	0.12	0.08
15-Jun-06	58.5	40.5	0.32	0.16	0.08
16-Jun-06	58.5	40.5	0.15	0.08	0.05
20-Jun-06	58.6	40.5	0.40	0.17	0.13
20-Jun-06	58.6	40.6	0.32	0.13	0.09
27-Jun-06	58.3	40.4	0.32	0.21	0.11
27-Jun-06	58.1	40.2	0.28	0.16	0.09
07-Jul-06	57.6	39.9	0.21	0.17	0.07
07-Jul-06	58.7	40.7	0.18	0.12	0.06
12-Jul-06	58.4	40.4	0.28	0.20	0.11
12-Jul-06	58.5	40.5	0.20	0.12	0.07
20-Jul-06	58.3	40.4	0.29	0.11	0.11
20-Jul-06	58.7	40.7	0.14	0.08	0.06
27-Jul-06	58.0	40.2	0.19	0.13	0.07
27-Jul-06	58.1	40.2	0.16	0.11	0.06
09-Aug-06	58.0	40.2	0.26	0.14	0.09
09-Aug-06	58.1	40.3	0.28	0.14	0.09
18-Aug-06	58.6	40.6	0.28	0.15	0.11
18-Aug-06	58.4	40.5	0.31	0.15	0.11
22-Aug-06	57.8	40.0	0.27	0.17	0.09
22-Aug-06	58.5	40.5	0.29	0.19	0.10
31-Aug-06	57.8	40.1	0.27	0.13	0.10
31-Aug-06	58.1	40.3	0.26	0.13	0.09
04-Sep-06	57.0	39.5	0.21	0.13	0.08
07-Sep-06	58.6	40.6	0.24	0.18	0.09
11-Sep-06	58.5	40.5	0.25	0.15	0.08
11-Sep-06	57.8	40.0	0.23	0.14	0.07
15-Sep-06	58.6	40.6	0.16	0.13	0.06
15-Sep-06	58.5	40.5	0.48	0.17	0.07
25-Sep-06	57.2	39.6	0.33	0.10	0.17
25-Sep-06	58.7	40.7	0.16	0.07	0.09
02-Oct-06	58.0	40.2	0.28	0.16	0.07
02-Oct-06	58.4	40.5	0.27	0.14	0.08
09-Oct-06	58.7	40.7	0.24	0.12	0.09
09-Oct-06	58.7	40.6	0.25	0.12	0.11
12-Oct-06	57.7	40.0	0.23	0.08	0.14
12-Oct-06	57.8	40.0	0.19	0.13	0.06
22-Oct-06	58.7	40.6	0.19	0.09	0.06
22-Oct-06	58.2	40.3	0.24	0.10	0.07
29-Oct-06	58.1	40.3	0.23	0.11	0.08
29-Oct-06	58.2	40.3	0.28	0.12	0.11

WTS-60 Dolime Feed Chemistry Summary 2004 to 2007 (contd)
(from Patterson 2007)

LOAD DATE	CAO	MGO	SIO2	FE2O3	AL2O3
04-Nov-06	58.0	40.2	0.23	0.12	0.08
09-Nov-06	57.9	40.1	0.15	0.11	0.06
12-Nov-06	58.2	40.3	0.14	0.09	0.05
12-Nov-06	58.0	40.1	0.16	0.09	0.06
23-Nov-06	58.6	40.5	0.24	0.10	0.08
23-Nov-06	58.6	40.6	0.21	0.11	0.08
30-Nov-06	57.8	40.0	0.17	0.09	0.06
30-Nov-06	58.1	40.3	0.39	0.17	0.15
01-Dec-06	58.6	40.6	0.34	0.17	0.09
02-Dec-06	58.4	40.4	0.28	0.10	0.05
13-Dec-06	58.5	40.5	0.29	0.18	0.10
13-Dec-06	58.2	40.3	0.32	0.14	0.09
22-Dec-06	58.2	40.3	0.24	0.10	0.08
20-Dec-06	58.5	40.5	0.28	0.16	0.10
26-Dec-06	58.4	40.5	0.29	0.18	0.10
26-Dec-06	58.6	40.6	0.29	0.19	0.09
02-Jan-07	58.7	40.7	0.26	0.08	0.08
02-Jan-07	57.5	39.8	0.31	0.08	0.06
09-Jan-07	58.2	40.3	0.17	0.09	0.07
07-Jan-07	57.7	40.0	0.23	0.10	0.08
18-Jan-07	58.6	40.6	0.12	0.07	0.05
19-Jan-07	57.9	40.1	0.12	0.06	0.03
23-Jan-07	58.2	40.3	0.30	0.21	0.09
25-Jan-07	58.6	40.6	0.19	0.16	0.07
27-Jan-07	58.4	40.5	0.33	0.15	0.11
28-Jan-07	58.0	40.2	0.32	0.15	0.09
06-Feb-07	58.3	40.4	0.32	0.11	0.08
06-Feb-07	58.6	40.6	0.34	0.12	0.09
16-Feb-07	57.8	40.0	0.30	0.18	0.10
16-Feb-07	58.5	40.5	0.35	0.22	0.13
22-Feb-07	58.2	40.3	0.31	0.15	0.12
22-Feb-07	58.3	40.4	0.34	0.20	0.13
01-Mar-07	58.5	40.5	0.31	0.16	0.11
02-Mar-07	58.5	40.5	0.34	0.20	0.12
06-Mar-07	57.9	40.1	0.25	0.12	0.09
06-Mar-07	57.8	40.0	0.41	0.19	0.12
17-Mar-07	58.6	40.6	0.28	0.15	0.10
17-Mar-07	58.7	40.6	0.24	0.14	0.09
20-Mar-07	58.4	40.5	0.25	0.17	0.11
20-Mar-07	58.6	40.6	0.29	0.15	0.09
27-Mar-07	58.5	40.5	0.42	0.19	0.12
28-Mar-07	58.6	40.6	0.43	0.17	0.11
03-Apr-07	58.3	40.4	0.79	0.13	0.11
03-Apr-07	58.5	40.5	0.39	0.15	0.12
13-Apr-07	58.4	40.4	0.27	0.11	0.10
13-Apr-07	58.5	40.5	0.23	0.10	0.08
18-Apr-07	58.3	40.3	0.46	0.28	0.22
17-Apr-07	58.1	40.2	0.44	0.24	0.18
27-Apr-07	58.4	40.5	0.44	0.23	0.17
27-Apr-07	58.5	40.5	0.37	0.19	0.15
04-May-07	57.5	39.9	0.37	0.16	0.14
05-May-07	57.8	40.0	0.24	0.11	0.08
11-May-07	58.5	40.5	0.24	0.10	0.09
12-May-07	58.5	40.5	0.22	0.11	0.08
14-May-07	57.7	40.0	0.39	0.24	0.14

WTS-60 Dolime Feed Chemistry Summary 2004 to 2007 (contd) (from Patterson 2007)

LOAD DATE	CAO	MGO	SIO2	FE2O3	AL2O3
14-May-07	58.5	40.5	0.24	0.18	0.10
25-May-07	58.7	40.6	0.18	0.09	0.06
25-May-07	58.6	40.6	0.25	0.12	0.09
29-May-07	58.5	40.5	0.16	0.10	0.06
31-May-07	58.3	40.4	0.27	0.13	0.10
07-Jun-07	58.8	40.7	0.16	0.12	0.08
07-Jun-07	58.1	40.3	0.23	0.13	0.10
AVERAGE	58.2	40.4	0.30	0.15	0.10
STD DEV	0.355	0.214	0.085	0.042	0.030
DATA POINTS	333	333	333	333	333

WTS-60 Chemical Composition Data (from Patterson 2007)

Statistical Summary of MagChem 10 WTS 60 From Martin Marietta for 06/01/2006 through 05/31/2007

	Chloride, as Cl, %	Iron , as Fe$_2$O$_3$, %	Loss On Ignition, %	Magnesium, as MgO, (on ignited basis) %	Aluminum , as Al$_2$O$_3$, %	Silicon, as SiO$_2$, %	Sulfur, as SO$_3$, %	Calcium , as CaO, %
Count	146	146	145	146	146	146	146	146
Average	0.0016589	0.154306	0.142414	98.4788	0.133954	0.347812	0.000341781	0.903901
2 Std. Dev	0.0183789	0.0292273	0.128398	0.169459	0.0139122	0.0883279	0.00282362	0.106868
Minimum	0	0.0842	0.01	98.0999	0.1069	0.1537	0	0.6221
Maximum	0.1052	0.1981	0.5	98.9057	0.1782	0.4271	0.011	1.1349
Average + Std. Dev	0.0200378	0.183533	0.270811	98.6483	0.147866	0.43614	0.0031654	1.01077
Average - Std. Dev	-0.01672	0.125079	0.0140163	98.3094	0.120042	0.259484	-0.00248184	0.797033

Statistical Summary of MagChem 10 WTS 60 From Martin Marietta for 12/01/2004 through 12/01/2005

	Chloride, as Cl, %	Iron , as Fe$_2$O$_3$, %	Loss On Ignition, %	Magnesium, as MgO, (on ignited basis) %	Aluminum , as Al$_2$O$_3$, %	Silicon, as SiO$_2$, %	Sulfur, as SO$_3$, %	Calcium , as CaO, %
Count	166	166	166	166	166	166	166	166
Average	0.000495783	0.161958	0.166084	98.4808	0.125189	0.348902	0	0.903758
2 Std. Dev	0.00913727	0.0223242	0.118695	0.166225	0.0235845	0.0754838	0	0.112036
Minimum	0	0.1331	0.06	98.2362	0.0996	0.24	0	0.7236
Maximum	0.0583	0.1961	0.34	98.7065	0.1988	0.5175	0	1.0581
Average + Std. Dev	0.00963305	0.184283	0.28478	98.647	0.148773	0.424386	0	1.01579
Average - Std. Dev	-0.00864148	0.139634	0.0473889	98.3146	0.101604	0.273419	0	0.791723